# Nanopore-based genome assembly and the evolutionary genomics of basmati rice

Jae Young Choi[1*], Zoe N. Lye[1], Simon C. Groen[1], Xiaoguang Dai[2], Priyesh Rughani[2], Sophie Zaaijer[3], Eoghan D. Harrington[2], Sissel Juul[2] and Michael D. Purugganan[1,4*]

[1]Center for Genomics and Systems Biology, Department of Biology, New York University, New York, New York, USA

[2]Oxford Nanopore Technologies, New York, New York, USA

[3]New York Genome Center, New York, New York, USA

[4]Center for Genomics and Systems Biology, NYU Abu Dhabi Research Institute, New York University Abu Dhabi, Abu Dhabi, United Arab Emirates

* Corresponding authors, Email: jyc387@nyu.edu (JYC), mp132@nyu.edu (MDP)

## ABSTRACT

### BACKGROUND

The *circum*-basmati group of cultivated Asian rice (*Oryza sativa*) contains many iconic varieties and is widespread in the Indian subcontinent. Despite its economic and cultural importance, a high-quality reference genome is currently lacking, and the group's evolutionary history is not fully resolved. To address these gaps, we used long-read nanopore sequencing and assembled the genomes of two *circum*-basmati rice varieties, Basmati 334 and Dom Sufid.

### RESULTS

We generated two high-quality, chromosome-level reference genomes that represented the 12 chromosomes of *Oryza*. The assemblies showed a contig N50 of 6.32Mb and 10.53Mb for Basmati 334 and Dom Sufid, respectively. Using our highly contiguous assemblies we characterized structural variations segregating across *circum*-basmati genomes. We discovered repeat expansions not observed in japonica—the rice group most closely related to *circum*-basmati—as well as presence/absence variants of over 20Mb, one of which was a *circum*-basmati-specific deletion of a gene regulating awn length. We further detected strong evidence of admixture between the *circum*-basmati and *circum*-aus groups. This gene flow had its greatest effect on chromosome 10, causing both structural variation and single nucleotide polymorphism to deviate from genome-wide history. Lastly, population genomic analysis of 78 *circum*-basmati varieties showed three major geographically structured genetic groups: (1) Bhutan/Nepal group, (2) India/Bangladesh/Myanmar group, and (3) Iran/Pakistan group.

### CONCLUSION

Availability of high-quality reference genomes from nanopore sequencing allowed functional and evolutionary genomic analyses, providing genome-wide evidence for gene flow between *circum*-aus and *circum*-basmati, the nature of *circum*-basmati structural variation, and the presence/absence of genes in this important and iconic rice variety group.

**KEYWORDS**

*Oryza sativa,* Asian rice, aromatic rice group, domestication, crop evolution, nanopore sequencing, aus, basmati, indica, japonica, admixture, awnless, *de novo* genome assembly

## BACKGROUND

*Oryza sativa* or Asian rice is an agriculturally important crop that feeds one-half of the world's population [1], and supplies 20% of people's caloric intake (www.fao.org). Historically, *O. sativa* has been classified into two major variety groups, japonica and indica, based on morphometric differences and molecular markers [2, 3]. These variety groups can be considered as subspecies, particularly given the presence of reproductive barriers between them [4]. Archaeobotanical remains suggest japonica rice was domesticated ~9,000 years ago in the Yangtze Basin of China, while indica rice originated ~4,000 years ago when domestication alleles were introduced from japonica into either *O. nivara* or a proto-indica in the Indian subcontinent [5]. More recently, two additional variety groups have been recognized that are genetically distinct from japonica and indica: the aus/*circum*-aus and aromatic/*circum*-basmati rices [6–8].

The rich genetic diversity of Asian rice is likely a result from a complex domestication process involving multiple wild progenitor populations and the exchange of important

domestication alleles between *O. sativa* variety groups through gene flow [5, 7, 9–17]. Moreover, many agricultural traits within rice are variety group-specific [18–23], suggesting local adaptation to environments or cultural preferences have partially driven the diversification of rice varieties.

Arguably, the *circum*-basmati rice group has been the least studied among the four major variety groups, and it was only recently defined in more detail based on insights from genomic data [7]. Among its members the group boasts the iconic basmati rices (*sensu stricto*) from southern Asia and the sadri rices from Iran [6]. Many, but not all, *circum*-basmati varieties are characterized by distinct and highly desirable fragrance and texture [24]. Nearly all fragrant *circum*-basmati varieties possess a loss-of-function mutation in the *BADH2* gene that has its origins in ancestral japonica haplotypes, suggesting that an introgression between *circum*-basmati and japonica may have led to fragrant basmati rice [21, 25, 26]. Genome-wide polymorphism analysis of a smaller array of *circum*-basmati rice cultivars shows close association with japonica varieties [7, 16, 27], providing evidence that at least part of the genomic make-up of *circum*-basmati rices may indeed be traced back to japonica.

Whole-genome sequences are an important resource for evolutionary geneticists studying plant domestication, as well as breeders aiming to improve crop varieties. Single-molecule sequencing regularly produces sequencing reads in the range of kilobases (kb) [28]. This is particularly helpful for assembling plant genomes, which are often highly repetitive and heterozygous, and commonly underwent at least one round of polyploidization in the past [29–31]. The *Oryza sativa* genome, with a relatively modest size of ~400 Mb, was the first crop genome sequence assembled [29], and there has been much progress in generating *de novo* genome assemblies for other members of the genus *Oryza*. Currently, there are assemblies for

nine wild species (*Leersia perrieri* [outgroup], *O. barthii*, *O. brachyantha*, *O. glumaepatula*, *O. longistaminata*, *O. meridionalis*, *O. nivara*, *O. punctata*, and *O. rufipogon*) and two domesticated species (*O. glaberrima* and *O. sativa*) [32–37].

Within domesticated Asian rice (*O. sativa*), genome assemblies are available for cultivars in most variety groups [32, 33, 38–42]. However, several of these reference assemblies are based on short-read sequencing data and show higher levels of incompleteness compared to assemblies generated from long-read sequences [40, 41]. Nevertheless, these *de novo* genome assemblies have been critical in revealing genomic variation (*e.g.* variations in genome structure and repetitive DNA, and *de novo* species- or population-specific genes) that were otherwise missed from analyzing a single reference genome. Recently, a genome assembly based on short-read sequencing data was generated for basmati rice [42]. Not only were there missing sequences in this assembly, it was also generated from DNA of an elite basmati breeding line. Such modern cultivars are not the best foundations for domestication-related analyses due to higher levels of introgression from other rice populations during modern breeding.

Here, we report the *de novo* sequencing and assembly of the landraces (traditional varieties) Basmati 334 [21, 43, 44] and Dom Sufid [21, 24, 45, 46] using the long-read nanopore sequencing platform of Oxford Nanopore Technologies [47]. Basmati 334 is from Pakistan, evolved in a rainfed lowland environment and is known to be drought tolerant at the seedling and reproductive stages [44]. It also possesses several broad-spectrum bacterial blight resistance alleles [48, 49], making Basmati 334 desirable for breeding resilience into modern basmati cultivars [49, 50]. Dom Sufid is an Iranian sadri cultivar that, like other sadri and basmati (*sensu stricto*) varieties, is among the most expensive varieties currently available in the market [24]. It has desirable characteristics such as aromaticity and grain elongation during cooking, although it

is susceptible to disease and abiotic stress [24, 51]. Because of their special characteristics, both Basmati 334 and Dom Sufid are used in elite rice breeding programs to create high yielding and resilient aromatic rice varieties [24, 44–46, 50].

Based on long reads from nanopore sequencing, our genome assemblies have high quality, contiguity, and genic completeness, making them comparable in quality to assemblies associated with key rice reference genomes. We used our *circum*-basmati genome assemblies to characterize genomic variation existing within this important rice variety group, and analyze domestication-related and other evolutionary processes that shaped this variation. Our *circum*-basmati rice genome assemblies will be valuable complements to the available assemblies for other rice cultivars, unlocking important genomic variation for rice crop improvement.

## RESULTS

**Nanopore sequencing of basmati and sadri rice.** Using Oxford Nanopore Technologies' long-read sequencing platform, we sequenced the genomes of the *circum*-basmati landraces Basmati 334 (basmati *sensu stricto*) and Dom Sufid (sadri). We called 1,372,950 reads constituting a total of 29.2 Gb for Basmati 334 and 1,183,159 reads constituting a total of 24.2 Gb for Dom Sufid (Table 1). For both samples the median read length was > 17 kb, the read length N50 was > 33 kb, and the median quality score per read was ~11.

**Table 1. Summary of nanopore sequencing read data**.

| Flow-cell | Number of Reads | Median Read Length | Read Length N50 | Median Quality Score (QS) | Total Bases |
|---|---|---|---|---|---|
| | | | Basmati 334 | | |

| | | | | | |
|---|---|---|---|---|---|
| FAK30515 | 288,473 | 19,905 | 36,743 | 11.27 | 6,843,069,570 |
| FAK30732 | 306,247 | 18,792 | 30,974 | 11.19 | 6,341,851,953 |
| FAK30522 | 228,191 | 17,366 | 36,456 | 11.07 | 4,816,938,523 |
| FAK27872 | 244,606 | 18,335 | 31,267 | 11.35 | 5,045,781,146 |
| FAK27919 | 305,433 | 18,087 | 30,727 | 11.43 | 6,191,306,294 |
| All | 1,372,950 | 18,576 | 33,005 | 11.27 | 29,238,947,486 |
| | | | Dom Sufid | | |
| FAK30464 | 300,290 | 18,477 | 37,754 | 11.34 | 6,681,819,859 |
| FAK30582 | 258,584 | 17,641 | 34,213 | 11.30 | 5,353,774,444 |
| FAK28890 | 330,924 | 16,756 | 34,033 | 10.96 | 6,553,200,184 |
| FAK30064 | 293,361 | 16,178 | 32,835 | 10.99 | 5,618,557,776 |
| All | 1,183,159 | 17,237 | 34,728 | 11.14 | 24,207,352,263 |

***De novo* assembly of the Basmati 334 and Dom Sufid rice genomes.** Incorporating only those reads that had a mean quality score of > 8 and read lengths of > 8 kb, we used a total of 1,076,192 reads and 902,040 reads for the Basmati 334 and Dom Sufid genome assemblies, which resulted in a genome coverage of ~62× and ~51×, respectively (Table 2). We polished the genome assemblies with both nanopore and short Illumina sequencing reads. The final, polished genome assemblies spanned 386.5 Mb across 188 contigs for Basmati 334, and 383.6 Mb across 116 contigs for Dom Sufid. The genome assemblies had high contiguity, with a contig N50 of 6.32 Mb and 10.53 Mb for Basmati 334 and Dom Sufid, respectively. Our genome assemblies recovered more than 97% of the 1,440 BUSCO [52] embryophyte gene groups, which is

147 comparable to the BUSCO statistics for the japonica Nipponbare [33] (98.4%) and indica R498
148 reference genomes [41] (98.0%). This is an improvement from the currently available genome
149 assembly of basmati variety GP295-1 [42], which was generated from Illumina short-read
150 sequencing data and has a contig N50 of 44.4 kb with 50,786 assembled contigs.

151 We examined coding sequences of our *circum*-basmati genomes by conducting gene
152 annotation using published rice gene models and the *MAKER* gene annotation pipeline [52, 53].
153 A total of 41,270 genes were annotated for the Basmati 334 genome, and 38,329 for the Dom
154 Sufid genome. BUSCO gene completion analysis [52] indicated that 95.4% and 93.6% of the
155 3,278 single copy genes from the liliopsida gene dataset were found in the Basmati 334 and Dom
156 Sufid gene annotations respectively.

157

158 **Table 2. Summary of the *circum*-basmati rice genome assemblies**

| | Basmati 334 | Dom Sufid |
|---|---|---|
| Genome Coverage | 62.5× | 51.4× |
| Number of Contigs | 188 | 116 |
| Total Number of Bases in Contigs | 386,555,741 | 383,636,250 |
| Total Number of Bases Scaffolded | 386,050,525 | 383,245,802 |
| Contig N50 Length | 6.32 Mb | 10.53 Mb |
| Contig L50 | 20 | 13 |
| Total Contigs > 50 kbp | 159 | 104 |
| Maximum Contig Length | 17.04 Mb | 26.82 Mb |
| BUSCO Gene Completion (Assembly) | 97.6% | 97.0% |
| GC Content | 43.6% | 43.7% |

| | | |
|---|---|---|
| Repeat Content | 44.4% | 44.2% |
| Number of Annotated Genes | 41,270 | 38,329 |
| BUSCO Gene Completion (Annotation) | 95.4% | 93.6% |

**Whole genome comparison to other rice variety group genomes.** We aligned our draft genome assemblies to the japonica Nipponbare reference genome sequence [33], which represents one of the highest quality reference genome sequences (Figure 1A). Between the Nipponbare, Basmati 334 and Dom Sufid genomes, high levels of macro-synteny were evident across the japonica chromosomes. Specifically, we observed little large-scale structural variation between Basmati 334 and Dom Sufid contigs and the japonica genome. A noticeable exception was an apparent inversion in the *circum*-basmati genome assemblies at chromosome 6 between positions 12.5 Mb and 18.7 Mb (Nipponbare coordinates), corresponding to the pericentromeric region [54]. Interestingly, the same region showed an inversion between the Nipponbare and indica R498 reference genomes [41], whereas in the *circum*-aus N22 cultivar no inversions are observed (Supplemental Figure 1). While the entire region was inverted in R498, the inversion positions were disjoint in Basmati 334 and Dom Sufid, apparently occurring in multiple regions of the pericentromere. We independently verified the inversions by aligning raw nanopore sequencing reads to the Nipponbare reference genome using the long read-aware aligner *ngmlr* [55], and the structural variation detection program *sniffles* [55]. *Sniffles* detected several inversions, including a large inversion between positions 13.1 and 17.7 Mb and between 18.18 and 18.23 Mb, with several smaller inversions located within the largest inversion (Supplemental Table 1).

Because of high macro-synteny with japonica (Figure 1A), we ordered and oriented the contigs of the Basmati 334 and Dom Sufid assemblies using a reference genome-based scaffolding approach [56]. For both Basmati 334 and Dom Sufid, over 99.9% of the assembled genomic contigs were anchored to the Nipponbare reference genome (Table 2). The scaffolded *circum*-basmati chromosomes were similar in size to those in reference genomes for cultivars in other rice variety groups (Nipponbare [33], the *circum*-aus variety N22 [37], and the indica varieties IR8 [37] and R498 [41]) that were sequenced, assembled, and scaffolded to near completion (Table 3).

**Table 3. Comparison of assembled chromosome sizes for cultivars across variety groups**.

| Chromosome | Basmati 334 | Dom Sufid | Nipponbare | N22 | IR8 | R498 |
|---|---|---|---|---|---|---|
| 1 | 44,411,451 | 44,306,286 | 43,270,923 | 44,711,178 | 44,746,683 | 44,361,539 |
| 2 | 35,924,761 | 36,365,206 | 35,937,250 | 38,372,633 | 37,475,564 | 37,764,328 |
| 3 | 40,305,655 | 38,133,813 | 36,413,819 | 36,762,248 | 39,065,119 | 39,691,490 |
| 4 | 34,905,232 | 34,714,597 | 35,502,694 | 33,558,078 | 35,713,470 | 35,849,732 |
| 5 | 30,669,872 | 31,017,353 | 29,958,434 | 28,792,057 | 31,269,760 | 31,237,231 |
| 6 | 29,982,228 | 32,412,977 | 31,248,787 | 29,772,976 | 32,072,649 | 32,465,040 |
| 7 | 30,410,531 | 29,511,326 | 29,697,621 | 29,936,233 | 30,380,234 | 30,277,827 |
| 8 | 29,921,941 | 29,962,976 | 28,443,022 | 25,527,801 | 30,236,384 | 29,952,003 |
| 9 | 24,050,083 | 23,970,096 | 23,012,720 | 22,277,206 | 24,243,884 | 24,760,661 |
| 10 | 25,596,481 | 24,989,786 | 23,207,287 | 20,972,683 | 25,246,678 | 25,582,588 |
| 11 | 29,979,012 | 29,949,236 | 29,021,106 | 29,032,419 | 32,337,678 | 31,778,392 |
| 12 | 29,893,278 | 27,912,150 | 27,531,856 | 22,563,585 | 25,963,606 | 26,601,357 |

| | | | | | | |
|---|---|---|---|---|---|---|
| Total | 386,050,525 | 383,245,802 | 373,245,519 | 362,279,097 | 388,751,709 | 390,322,188 |

Next, we assessed the assembly quality of the *circum*-basmati genomes by contrasting them against available *de novo*-assembled genomes within the Asian rice complex (see Materials and Method for a complete list of genomes). We generated a multi-genome alignment to the Nipponbare genome, which we chose as the reference since its assembly and gene annotation is a product of years of community-based efforts [33, 57, 58]. To infer the quality of the gene regions in each of the genome assemblies, we used the multi-genome alignment to extract the coding DNA sequence of each Nipponbare gene and its orthologous regions from each non-japonica genome. The orthologous genes were counted for missing DNA sequences ("N" sequences) and gaps to estimate the percent of Nipponbare genes covered. For all genomes the majority of Nipponbare genes had a near-zero proportion of sites that were missing in the orthologous non-Nipponbare genes (Supplemental Figure 2). The missing proportions of Nipponbare-orthologous genes within the Basmati 334 and Dom Sufid genomes were comparable to those for genomes that had higher assembly contiguity [37, 40, 41].

Focusing on the previously sequenced basmati GP295-1 genome [42], our newly assembled *circum*-basmati genomes had noticeably lower proportions of missing genes (Supplemental Figure 2). Furthermore, over 96% of base pairs across the Nipponbare genome were alignable against the Basmati 334 (total of 359,557,873 bp [96.33%] of Nipponbare genome) or Dom Sufid (total of 359,819,239 bp [96.40%] of Nipponbare genome) assemblies, while only 194,464,958 bp (52.1%) of the Nipponbare genome were alignable against the GP295-1 assembly.

We then counted the single-nucleotide and insertion/deletion (indel, up to ~60 bp) differences between the *circum*-basmati and Nipponbare assemblies to assess the overall quality of our newly assembled genomes. To avoid analyzing differences across unconstrained repeat regions, we specifically examined regions where there were 20 exact base-pair matches flanking a site that had a single nucleotide or indel difference between the *circum*-basmati and Nipponbare genomes. In the GP295-1 genome there were 334,500 (0.17%) single-nucleotide differences and 44,609 (0.023%) indels compared to the Nipponbare genome. Our newly assembled genomes had similar proportions of single-nucleotide differences with the Nipponbare genome, where the Basmati 334 genome had 780,735 (0.22%) differences and the Dom Sufid genome had 731,426 (0.20%). For indels the Basmati 334 genome had comparable proportions of differences with 104,282 (0.029%) variants, but the Dom Sufid genome had higher proportions with 222,813 (0.062%) variants. In sum, our draft *circum*-basmati genomes had high contiguity and completeness as evidenced by assembly to the chromosome level, and comparison to the Nipponbare genome. In addition, our genome assemblies were comparable to the Illumina sequence-generated GP295-1 genome for the proportion of genomic differences with the Nipponbare genome, suggesting they had high quality and accuracy as well.

Our *circum*-basmati genome assemblies should also be of sufficiently high quality for detailed gene-level analysis. For instance, a hallmark of many *circum*-basmati rices is aromaticity, and a previous study had determined that Dom Sufid, but not Basmati 334, is a fragrant variety [21]. We examined the two genomes to verify the presence or absence of the mutations associated with fragrance. There are multiple different loss-of-function mutations in the *BADH2* gene that cause rice varieties to be fragrant [21, 25, 26], but the majority of fragrant rices carry a deletion of 8 nucleotides at position chr8:20,382,861-20,382,868 of the Nipponbare

genome assembly (version Os-Nipponbare-Reference-IRGSP-1.0). Using the genome alignment, we extracted the *BADH2* sequence region to compare the gene sequence of the non-fragrant Nipponbare to that of Basmati 334 and Dom Sufid. Consistent with previous observations [21], we found that the genome of the non-fragrant Basmati 334 did not carry the deletion and contained the wild-type *BADH2* haplotype observed in Nipponbare. The genome of the fragrant Dom Sufid, on the other hand, carried the 8-bp deletion, as well as the 3 single-nucleotide polymorphisms flanking the deletion. This illustrates that the Basmati 334 and Dom Sufid genomes are accurate enough for gene-level analysis.

***Circum*-basmati gene analysis.** Our annotation identified ~40,000 coding sequences in the *circum*-basmati assemblies. We examined population frequencies of the annotated gene models across a *circum*-basmati population dataset to filter out mis-annotated gene models or genes at very low frequency in a population. We obtained Illumina sequencing reads from varieties included in the 3K Rice Genome Project [7] and sequenced additional varieties to analyze a total of 78 *circum*-basmati cultivars (see Supplemental Table 2 for a list of varieties). The Illumina sequencing reads were aligned to the *circum*-basmati genomes, and if the average coverage of a genic region was < 0.05× for an individual this gene was called as a deletion in that variety. Since we used a low threshold for calling a deletion, the genome-wide sequencing coverage of a variety did not influence the number of gene deletions detected (Supplemental Figure 3). Results showed that gene deletions were indeed rare across the *circum*-basmati population (Figure 2A), consistent with their probable deleterious nature. We found that 31,565 genes (76.5%) in Basmati 334 and 29,832 genes (77.8%) in the Dom Sufid genomes did not have a deletion across the population (see Supplemental Table 3 for a list of genes).

There were 517 gene models from Basmati 334 and 431 gene models from Dom Sufid that had a deletion frequency of ≥ 0.3 (see Supplemental Table 4 for a list of genes). These gene models with high deletion frequencies were not considered further in this analysis. The rest were compared against the *circum*-aus N22, indica R498, and japonica Nipponbare gene models to determine their orthogroup status (Figure 2B; see Supplemental Table 5 for a list of genes and their orthogroup status), which are sets of genes that are orthologs and recent paralogs of each other [59].

The most frequent orthogroup class observed was for groups in which every rice variety group has at least one gene member. There were 13,894 orthogroups within this class, consisting of 17,361 genes from N22, 18,302 genes from Basmati 334, 17,936 genes from Dom Sufid, 17,553 genes from R498, and 18,351 genes from Nipponbare. This orthogroup class likely represents the set of core genes of *O. sativa* [42]. The second-highest orthogroup class observed was for groups with genes that were uniquely found in both *circum*-basmati genomes (3,802 orthogroups). These genes represent those restricted to the *circum*-basmati group.

In comparison to genes in other rice variety groups, the *circum*-basmati genes shared the highest number of orthogroups with *circum*-aus (2,648 orthogroups), followed by japonica (1,378 orthogroups), while sharing the lowest number of orthogroups with indica (663 orthogroups). In fact, genes from indica variety R498 had the lowest number assigned to an orthogroup (Figure 2B inset table), suggesting this genome had more unique genes, *i.e.* without orthologs/paralogs to genes in other rice variety groups.

**Genome-wide presence/absence variation within the *circum*-basmati genomes.** Our assembled *circum*-basmati genomes were >10 Mb longer than the Nipponbare genome, but

individual chromosomes showed different relative lengths (Table 3) suggesting a considerable number of presence/absence variants (PAVs) between the genomes. We examined the PAVs between the *circum*-basmati and Nipponbare genomes using two different computational packages: (i) *sniffles*, which uses raw nanopore reads aligned to a reference genome to call PAVs, and (ii) *assemblytics* [60], which aligns the genome assemblies to each other and calls PAVs. The results showed that, while the total number of PAVs called by *sniffles* and *assemblytics* were similar, only ~36% of PAVs had overlapping positions (Table 4). In addition, the combined total size of PAVs was larger for predictions made by *sniffles* compared to those by *assemblytics*. For subsequent analysis we focused on PAVs that were called by both methods.

**Table 4. Comparison of presence/absence variation called by two different computational packages**.

| | *sniffles* | *assemblytics* | overlap |
|---|---|---|---|
| | | Basmati 334 | |
| Deletion Counts | 11,989 | 11,247 | 4051 |
| Deleted Basepairs | 43,768,763 | 29,048,238 | 19,328,854 |
| Insertion Counts | 11,447 | 12,161 | 3734 |
| Inserted Basepairs | 19,650,518 | 14,498,550 | 5,783,551 |
| | | Dom Sufid | |
| Deletion Counts | 9901 | 10,115 | 3649 |
| Deleted Basepairs | 36,600,114 | 26,128,143 | 17,274,967 |
| Insertion Counts | 9834 | 11,134 | 3340 |
| Inserted Basepairs | 16,527,995 | 12,902,410 | 5,160,503 |

The distribution of PAV sizes indicated that large PAVs were rare across the *circum*-basmati genomes, while PAVs < 500 bps in size were the most common (Figure 3A). Within smaller-sized PAVs those in the 200-500 bp size range showed a peak in abundance. A closer examination revealed that sequence positions of more than 75% of these 200-500 bp-sized PAVs overlapped with transposable element coordinates in the *circum*-basmati genomes (Supplemental Table 6). A previous study based on short-read Illumina sequencing data reported a similar enrichment of short repetitive elements such as the long terminal repeats (LTRs) of retrotransposons, *Tc1/mariner* elements, and *mPing* elements among PAVs in this size range [61].

PAVs shorter than 200 bps also overlapped with repetitive sequence positions in the *circum*-basmati genomes, but the relative abundance of each repeat type differed among insertion and deletion variants. Insertions in the Basmati 334 and Dom Sufid genomes had a higher relative abundance of simple sequence repeats (*i.e.* microsatellites) compared to deletions (Supplemental Table 6). These inserted simple sequence repeats were highly enriched for $(AT)_n$ dinucleotide repeats, which in Basmati 334 accounted for 66,624 bps out of a total of 72,436 bps (92.0%) of simple sequence repeats, and for Dom Sufid 56,032 bps out of a total of 63,127 bps (88.8%).

Between the Basmati 334 and Dom Sufid genomes, ~45% of PAVs had overlapping genome coordinates (Figure 3B) suggesting that variety-specific insertion and deletion polymorphisms were common. We plotted PAVs for each of our *circum*-basmati genomes to visualize their distribution (Figure 3C). Chromosome-specific differences in the distribution of PAVs were seen for each *circum*-basmati genome: in Basmati 334, for example, chromosome 1

had the lowest density of PAVs, while in Dom Sufid this was the case for chromosome 2 (Supplemental Figure 5). On the other hand, both genomes showed significantly higher densities of PAVs on chromosome 10 (Tukey's range test $P < 0.05$). This suggested that, compared to Nipponbare, chromosome 10 was the most differentiated in terms of insertion and deletion variations in both of our *circum*-basmati genomes.

**Evolution of *circum*-basmati rice involved group-specific gene deletions.** The proportion of repeat sequences found within the larger-sized PAVs (*i.e.* those > 2 kb) was high, where between 84% and 98% of large PAVs contained transposable element-related sequences (Supplemental Table 6). Regardless, these larger PAVs also involved loss or gain of coding sequences. For instance, gene ontology analysis of domesticated rice gene orthogroups showed enrichment for genes related to electron transporter activity among both *circum*-basmati-specific gene losses and gains (see Supplemental Table 7 for gene ontology results for *circum*-basmati-specific gene losses and Supplemental Table 8 for gene ontology results for *circum*-basmati-specific gene gains).

Many of these genic PAVs could have been important during the rice domestication process [11]. Gene deletions, in particular, are more likely to have a functional consequence than single-nucleotide polymorphisms or short indels and may underlie drastic phenotypic variation. In the context of crop domestication and diversification this could have led to desirable phenotypes in human-created agricultural environments. For instance, several domestication phenotypes in rice are known to be caused by gene deletions [35, 62–66].

There were 873 gene orthogroups for which neither of the *circum*-basmati genomes had a gene member, but for which genomes for all three other rice variety groups (N22, Nipponbare,

and R498) had at least one gene member. Among these, there were 545 orthogroups for which N22, Nipponbare, and R498 each had a single-copy gene member, suggesting that the deletion of these genes in both the Basmati 334 and Dom Sufid genomes could have had a major effect in *circum*-basmati. We aligned Illumina sequencing data from our *circum*-basmati population dataset to the japonica Nipponbare genome, and calculated deletion frequencies of Nipponbare genes that belonged to the 545 orthogroups (see Supplemental Table 9 for gene deletion frequencies in the *circum*-basmati population for the Nipponbare genes that are missing in Basmati 334 and Dom Sufid). The vast majority of these Nipponbare genes (509 orthogroups or 93.4%) were entirely absent in the *circum*-basmati population, further indicating that these were *circum*-basmati-specific gene deletions fixed within this variety group.

One of the genes specifically deleted in *circum*-basmati rice varieties was *Awn3-1* (Os03g0418600), which was identified in a previous study as associated with altered awn length in japonica rice [67]. Reduced awn length is an important domestication trait that was selected for ease of harvesting and storing rice seeds [68]. This gene was missing in both *circum*-basmati genomes and no region could be aligned to the Nipponbare *Awn3-1* genic region (Figure 2C). Instead of the *Awn3-1* coding sequence, this genomic region contained an excess of transposable element sequences, suggesting an accumulation of repetitive DNA may have been involved in this gene's deletion. The flanking arms upstream and downstream of Os03g0418600 were annotated in both *circum*-basmati genomes and were syntenic to the regions in both Nipponbare and N22. These flanking arms, however, were also accumulating transposable element sequences, indicating that this entire genomic region may be degenerating in both *circum*-basmati rice genomes.

**Repetitive DNA and retrotransposon dynamics in the *circum*-basmati genomes.** Repetitive DNA makes up more than 44% of the Basmati 334 and Dom Sufid genome assemblies (Table 2). Consistent with genomes of other plant species [69] the repetitive DNA was largely composed of Class I retrotransposons, followed by Class II DNA transposons (Figure 4A). In total, 171.1 Mb were annotated as repetitive for Basmati 334, and 169.5 Mb for Dom Sufid. The amount of repetitive DNA in the *circum*-basmati genomes was higher than in the Nipponbare (160.6 Mb) and N22 genomes (152.1 Mb), but lower than in the indica R498 (175.9 Mb) and IR8 (176.0 Mb) genomes. These differences in the total amount of repetitive DNA were similar to overall genome assembly size differences (Table 3), indicating that variation in repeat DNA accumulation is largely driving genome size differences in rice [70].

We focused our attention on retrotransposons, which made up the majority of the rice repetitive DNA landscape (Figure 4A). Using *LTRharvest* [71, 72], we identified and *de novo*-annotated LTR retrotransposons in the *circum*-basmati genomes. *LTRharvest* annotated 5,170 and 5,150 candidate LTR retrotransposons in Basmati 334 and Dom Sufid, respectively (Supplemental Tables 10 and 11). Of these, 4,180 retrotransposons (80.9% of all candidate LTR retrotransposons) in Basmati 334 and 4,228 (82.1%) in Dom Sufid were classified as LTR retrotransposons by *RepeatMasker*'s *RepeatClassifer* tool (http://www.repeatmasker.org). Most LTR retrotransposons were from the *gypsy* and *copia* superfamilies [73, 74], which made up 77.1% (3,225 *gypsy* elements) and 21.9% (915 *copia* elements) of LTR retrotransposons in the Basmati 334 genome, and 76.4% (3,231 *gypsy* elements) and 22.8% (962 *copia* elements) of LTR retrotransposons in the Dom Sufid genome, respectively. Comparison of LTR retrotransposon content among reference genomes from different rice variety groups (Supplemental Figure 4) revealed that genomes assembled to near completion (*i.e.* Nipponbare,

382 N22, Basmati 334, Dom Sufid, and indica varieties IR8 and R498, as well as MH63 and ZS97
383 [40]) had higher numbers of annotated retrotransposons than genomes generated from short-read
384 sequencing data (GP295-1, *circum*-aus varieties DJ123 [38] and Kasalath [39], and indica variety
385 IR64 [38]), suggesting genome assemblies from short-read sequencing data may be missing
386 certain repetitive DNA regions.

387 Due to the proliferation mechanism of LTR transposons, the DNA divergence of an LTR
388 sequence can be used to approximate the insertion time for an LTR retrotransposon [75].
389 Compared to other rice reference genomes, the insertion times for the Basmati 334 and Dom
390 Sufid LTR retrotransposons were most similar to those observed for elements in the *circum*-aus
391 N22 genome (Supplemental Figure 4). Within our *circum*-basmati assemblies, the *gypsy*
392 superfamily elements had a younger average insertion time (~2.2 million years ago) than
393 elements of the *copia* superfamily (~2.7 million years ago; Figure 4B).

394 Concentrating on *gypsy* and *copia* elements with the *rve* (integrase; Pfam ID: PF00665)
395 gene, we examined the evolutionary dynamics of these LTR retrotransposons by reconstructing
396 their phylogenetic relationships across reference genomes for the four domesticated rice variety
397 groups (N22, Basmati 334, Dom Sufid, R498, IR8, and Nipponbare), and the two wild rice
398 species (*O. nivara* and *O. rufipogon*; Fig 3C). The retrotransposons grouped into distinct
399 phylogenetic clades, which likely reflect repeats belonging to the same family or subfamily [76].
400 The majority of phylogenetic clades displayed short external and long internal branches,
401 consistent with rapid recent bursts of transposition observed across various rice LTR
402 retrotransposon families [77].

403 The *gypsy* and *copia* superfamilies each contained a clade in which the majority of
404 elements originated within *O. sativa*, present only among the four domesticated rice variety

groups (Figure 4C, single star; see Supplemental Tables 12 and 13 for their genome coordinates). Elements in the *gypsy* superfamily phylogenetic clade had sequence similarity (963 out of the 1,837 retrotransposons) to elements of the *hopi* family [78], while elements in the *copia* superfamily phylogenetic clade had sequence similarity (88 out of the 264) to elements in the *osr4* family [79]. Elements of the *hopi* family are found in high copy number in genomes of domesticated rice varieties [80] and this amplification has happened recently [81].

Several retrotransposon clades were restricted to certain rice variety groups. The *gypsy* superfamily harbored a phylogenetic clade whose elements were only present in genomes of *circum*-aus, *circum*-basmati, and indica varieties (Figure 4C, double star; see Supplemental Table 14 for their genome coordinates), while we observed a clade comprised mostly of *circum*-basmati-specific elements within the *copia* superfamily (Figure 4C, triple star; see Supplemental Table 15 for their genome coordinates). Only a few members of the *gypsy*-like clade had sequence similarity (7 out of 478) to elements of the *rire3* [82] and *rn215* [83] families. Members of both families are known to be present in high copy numbers in genomes of domesticated rice varieties, but their abundance differs between the japonica and indica variety groups [80], suggesting a *rire3*- or *rn215*-like element expansion in the *circum*-aus, *circum*-basmati, and indica genomes. A majority of the *circum*-basmati-specific *copia*-like elements had sequence similarity (109 out of 113) to members of the *houba* family [78], which are found in high copy numbers in certain individuals, but in lower frequency across the rice population [80]. This suggests the *houba* family might have undergone a recent expansion specifically within the *circum*-basmati genomes.

**Phylogenomic analysis on the origins of *circum*-basmati rice.** We estimated the phylogenetic relationships within and between variety groups of domesticated Asian rice. Our maximum-likelihood phylogenetic tree, based on four-fold degenerate sites from the Nipponbare coding sequences (Figure 5A), showed that each cultivar was monophyletic with respect to its variety group of origin. In addition, the *circum*-basmati group was sister to japonica rice, while the *circum*-aus group was sister to indica. Consistent with previous observations, the wild rices *O. nivara* and *O. rufipogon* were sister to the *circum*-aus and japonica rices, respectively [14]. While this suggests that each domesticated rice variety group may have had independent wild progenitors of origin, it should be noted that recent hybridization between wild and domesticated rice [84, 85] could lead to similar phylogenetic relationships.

To further investigate phylogenetic relationships between *circum*-basmati and japonica, we examined phylogenetic topologies of each gene involving the trio Basmati 334, Nipponbare, and *O. rufipogon*. For each gene we tested which of three possible topologies for a rooted three-species tree - *i.e.* [(P1, P2), P3], O, where O is outgroup *O. barthii* and P1, P2, and P3 are Basmati 334 (or Dom Sufid), Nipponbare, and *O. rufipogon*, respectively - were found in highest proportion. For the trio involving Basmati 334, Nipponbare, and *O. rufipogon* there were 7,581 genes (or 32.6%), and for the trio involving Dom Sufid, Nipponbare, and *O. rufipogon* there were 7,690 genes (or 33.1%), that significantly rejected one topology over the other two using an Approximately Unbiased (AU) topology test [86]. In both trios, the majority of those genes supported a topology that grouped *circum*-basmati and Nipponbare as sister to each other (Figure 5B; 3,881 [or 51.2%] and 4,407 [or 57.3%] genes for Basmati 334 and Dom Sufid, respectively). A lower number of genes (3,018 [or 39.8%] and 2,508 [or 32.6%] genes for Basmati 334 and

449 Dom Sufid, respectively) supported the topology that placed Nipponbare and *O. rufipogon*
450 together.

451 The topology test result suggested that [(japonica, *circum*-basmati), *O. rufipogon*] was
452 the true species topology, while the topology [(japonica, *O. rufipogon*), *circum*-basmati)]
453 represented possible evidence of admixture (although it could also arise from incomplete lineage
454 sorting). To test for introgression, we employed D-statistics from the ABBA-BABA test [87, 88].
455 The D-statistics for the topology [(japonica, *circum*-basmati), *O. rufipogon*] were significantly
456 negative - Figure 5C left panel; z-score = -14.60 and D ± s.e = -0.28 ± 0.019 for topology
457 [(Nipponbare, Basmati 334), *O. rufipogon*], and z-score = -9.09 and D = -0.20 ± 0.022 for
458 topology [(Nipponbare, Dom Sufid), *O. rufipogon*] - suggesting significant evidence of
459 admixture between japonica and *O. rufipogon*.

460 Our initial topology test suggested that the trio involving Dom Sufid, Nipponbare, and *O.*
461 *rufipogon* had a higher proportion of genes supporting the [(*circum*-basmati, japonica), *O.*
462 *rufipogon*] topology compared to the trio involving Basmati 334, Nipponbare, and *O. rufipogon*
463 (Figure 5B). This suggested within-population variation in the amount of japonica or *O.*
464 *rufipogon* ancestry across the *circum*-basmati genomes due to differences in gene flow. We
465 conducted ABBA-BABA tests involving the topology [(Basmati 334, Dom Sufid), Nipponbare
466 or *O. rufipogon*] to examine the differences in introgression between the *circum*-basmati and
467 japonica or *O. rufipogon* genomes. The results showed significantly positive D-statistics for the
468 topology [(Basmati 334, Dom Sufid), Nipponbare] (Figure 5C left panel; z-score = 8.42 and D =
469 0.27 ± 0.032), indicating that Dom Sufid shared more alleles with japonica than Basmati 334 did
470 due to a history of more admixture with japonica. The D-statistics involving the topology
471 [(Basmati 334, Dom Sufid), *O. rufipogon*] were also significantly positive (Figure 5C left panel;

z-score = 5.57 and D = 0.21 ± 0.038). While this suggests admixture between Dom Sufid and *O. rufipogon*, it may also be an artifact due to the significant admixture between japonica and *O. rufipogon*.

**Signatures of admixture between *circum*-basmati and *circum*-aus rice genomes.** Due to extensive admixture between rice variety group genomes [14] we examined whether the basmati genome was also influenced by gene flow with other divergent rice variety groups (*i.e. circum*-aus or indica rices). A topology test was conducted for a rooted, three-population species tree. For the trio involving Basmati 334, *circum*-aus variety N22, and indica variety R498 there were 7,859 genes (or 35.3%), and for the trio involving Dom Sufid, N22, and R498 there were 8,109 genes (or 37.8%), that significantly rejected one topology over the other two after an AU test. In both trios, more than half of the genes supported the topology grouping *circum*-aus and indica as sisters (Figure 5D). In addition, more genes supported the topology grouping *circum*-aus and *circum*-basmati as sisters than the topology grouping indica and *circum*-basmati as sisters. This suggested that the *circum*-aus variety group might have contributed a larger proportion of genes to *circum*-basmati through gene flow than the indica variety group did.

To test for evidence of admixture, we conducted ABBA-BABA tests involving trios of the *circum*-basmati, N22, and R498 genomes. Results showed significant evidence of gene flow between *circum*-aus and both *circum*-basmati genomes - Figure 5C, right panel; z-score = 5.70 and D = 0.082 ± 0.014 for topology [(R498, N22), Basmati 334]; and z-score = 8.44 and D = 0.11 ± 0.013 for topology [(R498, N22), Dom Sufid]. To test whether there was variability in the *circum*-aus or indica ancestry in each of the *circum*-basmati genomes, we conducted ABBA-BABA tests for the topology [(Basmati 334, Dom Sufid), N22 or R498]. Neither of the ABBA-

BABA tests involving the topology [(Basmati 334, Dom Sufid), N22] (Figure 5C, right panel; z-score = 1.20 and D = 0.025 ± 0.021) or the topology [(Basmati 334, Dom Sufid), R498) (Figure 5C, right panel; z-score = -2.24 and D = -0.06 ± 0.026) was significant, suggesting the amount of admixture from *circum*-aus to each of the two *circum*-basmati genomes was similar.

In sum, the phylogenomic analysis indicated that *circum*-basmati and japonica share the most recent common ancestor, while *circum*-aus has admixed with *circum*-basmati during its evolutionary history (Figure 5F). We then examined whether admixture from *circum*-aus had affected each of the *circum*-basmati chromosomes to a similar degree. For both *circum*-basmati genomes most chromosomes had D-statistics that were not different from the genome-wide D-statistics value or from zero (Figure 5E). Exceptions were chromosomes 10 and 11, where the bootstrap D-statistics were significantly higher than the genome-wide estimate.

**Population analysis on the origin of *circum*-basmati rice.** Since our analysis was based on single representative genomes from each rice variety group, we compared the results of our phylogenomic analyses to population genomic patterns in an expanded set of rice varieties from different groups. We obtained high coverage (>14×) genomic re-sequencing data (generated with Illumina short-read sequencing) from landrace varieties in the 3K Rice Genome Project [7] and from *circum*-basmati rice landraces we re-sequenced. In total, we analyzed 24 *circum*-aus, 18 *circum*-basmati, and 37 tropical japonica landraces (see Supplemental Table 16 for variety names). The raw Illumina sequencing reads were aligned to the scaffolded Basmati 334 genome and computationally genotyped. A total of 4,594,290 polymorphic sites were called across the three rice variety groups and used for further analysis.

517 To quantify relationships between *circum*-aus, *circum*-basmati, and japonica, we
518 conducted a topology-weighting analysis [89]. For three populations there are three possible
519 topologies and we conducted localized sliding window analysis to quantify the number of unique
520 sub-trees that supported each tree topology. Consistent with the phylogenomic analysis results,
521 the topology weight was largest for the topology that grouped japonica and *circum*-basmati as
522 sisters (Figure 6A; topology weight = 0.481 with 95% confidence interval [0.479-0.483]). The
523 topology that grouped *circum*-aus and *circum*-basmati together as sisters weighed significantly
524 more (topology weight = 0.318 with 95% confidence interval [0.316-0.320]) than the topology
525 that grouped japonica and *circum*-aus as sisters (topology weight = 0.201 with 95% confidence
526 interval [0.199-0.203). This was consistent with the admixture results from the comparative
527 phylogenomic analysis, which detected evidence of gene flow between *circum*-aus and *circum*-
528 basmati.
529 We then examined topology weights for each individual chromosome, since the ABBA-
530 BABA tests using the genome assemblies had detected variation in *circum*-aus ancestry between
531 different chromosomes (Figure 5E). The results showed that for most of the chromosomes the
532 topology [(japonica, *circum*-basmati), *circum*-aus] always weighed more than the remaining two
533 topologies. An exception was observed for chromosome 10 where the topology weight grouping
534 *circum*-aus and *circum*-basmati as sisters was significantly higher (topology weight = 0.433 with
535 95% confidence interval [0.424-0.442]) than the weight for the genome-wide topology that
536 grouped japonica and *circum*-basmati as sisters (topology weight = 0.320 with 95% confidence
537 interval [0.312-0.328]). This change in predominant topology was still observed when the
538 weights were calculated across wider local windows (Supplemental Figure 6). Another exception
539 could be seen for chromosome 6 where the genome-wide topology [(japonica, *circum*-basmati),

*circum*-aus] (topology weight = 0.367 with 95% confidence interval [0.359-0.374) and the admixture topology [*circum*-aus, *circum*-basmati), japonica] (topology weight = 0.355 with 95% confidence interval [0.349-0.362]) had almost equal weights. In larger window sizes the weight of the admixed topology was slightly higher than that of the genome-wide topology (Supplemental Figure 6).

To estimate the evolutionary/domestication scenario that might explain the observed relationships between the *circum*-aus, *circum*-basmati, and japonica groups, we used the diffusion-based approach of the program *δaδi* [90] and fitted specific demographic models to the observed allele frequency spectra for the three rice variety groups. Because all three rice groups have evidence of admixture with each other [7, 9, 14, 16] we examined 13 demographic scenarios involving symmetric, asymmetric, and "no migration" models between variety groups, with and without recent population size changes (Supplemental Figure 7). To minimize the effect of genetic linkage on the demography estimation, polymorphic sites were randomly pruned in 200 kb windows, resulting in 1,918 segregating sites. The best-fitting demographic scenario was one that modeled a period of lineage splitting and isolation, while gene flow only occurred after formation of the three populations and at a later time (Figure 6C; visualizations of the 2D site frequency spectrum and model fit can be seen in Supplemental Figure 8). This best-fitting model was one of the lesser-parameterized models we tested, and the difference in Akaike Information Criterion (ΔAIC) with the model with the second-highest likelihood was 25.46 (see Supplemental Table 17 for parameter estimates and maximum likelihood estimates for each demographic model).

562 **Genetic structure within the *circum*-basmati group.** We used the *circum*-basmati population
563 genomic data for the 78 varieties aligned to the scaffolded Basmati 334 genome, and called the
564 polymorphic sites segregating within this variety group. After filtering, a total of 4,430,322 SNPs
565 across the *circum*-basmati dataset remained, which were used to examine population genetic
566 relationships within *circum*-basmati.

567 We conducted principal component analysis (PCA) using the polymorphism data and
568 color-coded each *circum*-basmati rice variety according to its country of origin (Figure 7A). The
569 PCA suggested that *circum*-basmati rices could be divided into three major groups with clear
570 geographic associations: (Group 1) a largely Bhutan/Nepal-based group, (Group 2) an
571 India/Bangladesh/Myanmar-based group, and (Group 3) an Iran/Pakistan-based group. The rice
572 varieties that could not be grouped occupied an ambiguous space across the principal
573 components, suggesting these might represent admixed rice varieties.

574 To obtain better insight into the ancestry of each rice variety, we used *fastSTRUCTURE*
575 [91] and varied assumed ancestral population (K) from 2 to 5 groups so the ancestry proportion
576 of each rice variety could be estimated (Figure 7B). At K=2, the India/Bangladesh/Myanmar and
577 Iran/Pakistan rice groups were shown to have distinct ancestral components, while the
578 Bhutan/Nepal group was largely an admixture of the other two groups. At K=3, the grouping
579 status designated from the PCA was largely concordant with the ancestral components. At K=4,
580 most India/Bangladesh/Myanmar rices had a single ancestral component, but Iran/Pakistan rices
581 had two ancestral components that were shared with several Bhutan/Nepal landraces.
582 Furthermore, several of the cultivars from the latter group seemed to form an admixed group
583 with India/Bangladesh/Myanmar varieties. In fact, when a phylogenetic tree was reconstructed
584 using the polymorphic sites, varieties within the India/Bangladesh/Myanmar and Iran/Pakistan

groups formed a monophyletic clade with each other. On the other hand, Bhutan/Nepal varieties formed a paraphyletic group where several clustered with the Iran/Pakistan varieties (Supplemental Figure 9).

In summary, the *circum*-basmati rices have evolved across a geographic gradient with at least three genetic groups (Figure 7C). These existed as distinct ancestral groups that later admixed to form several other *circum*-basmati varieties. Group 1 and Group 3 rices in particular may have experienced greater admixture, while the Group 2 landraces remained genetically more isolated from other *circum*-basmati subpopulations. We also found differences in agronomic traits associated with our designated groups (Figure 7D). The grain length to width ratio, which is a highly prized trait in certain *circum*-basmati rices [24], was significantly larger in Group 3 Iran/Pakistan varieties. The thousand-kernel weights, on the other hand, were highest for Group 2 India/Bangladesh/Myanmar varieties and were significantly higher than those for the ungrouped and Group 1 Bhutan/Nepal varieties.

## DISCUSSION

Nanopore sequencing is becoming an increasingly popular approach to sequence and assemble the often large and complex genomes of plants [92–94]. Here, using long-read sequences generated with Oxford Nanopore Technologies' sequencing platform, we assembled genomes of two *circum*-basmati rice cultivars, with quality metrics that were comparable to other rice variety group reference genome assemblies [37, 40, 41]. With modest genome coverage, we were able to develop reference genome assemblies that represented a significant improvement over a previous *circum*-basmati reference genome sequence, which had been assembled with a > 3-fold higher genome coverage than ours, but from short-read sequences [42]. With additional

608 short-read sequencing reads, we were able to correct errors from the nanopore sequencing reads,
609 resulting in two high-quality *circum*-basmati genome assemblies.

610 Even with long-read sequence data, developing good plant reference genome sequences
611 still requires additional technologies such as optical mapping or Hi-C sequencing for improving
612 assembly contiguity [95–98], which can be error prone as well [56]. Our assemblies were also
613 fragmented into multiple contigs, but sizes of these contigs were sufficiently large that we could
614 use reference genome sequences from another rice variety group to anchor the majority of
615 contigs and scaffold them to higher-order chromosome-level assemblies. Hence, with a highly
616 contiguous draft genome assembly, reference genome-based scaffolding can be a cost-efficient
617 and powerful method of generating chromosome-level assemblies.

618 Repetitive DNA constitutes large proportions of plant genomes [99], and there is an
619 advantage to using long-read sequences for genome assembly as it enables better annotation of
620 transposable elements. Many transposable element insertions have evolutionarily deleterious
621 consequences in the rice genome [54, 100, 101], but some insertions could have beneficial
622 effects on the host [102]. Using our genome assembly, we have identified retrotransposon
623 families that have expanded specifically within *circum*-basmati genomes. While more study will
624 be necessary to understand the functional effects of these insertions, long-read sequences have
625 greatly improved the assembly and identification of repeat types.

626 Due to a lack of archaeobotanical data, the origins of *circum*-basmati rice have remained
627 elusive. Studies of this variety group's origins have primarily focused on genetic differences that
628 exist between *circum*-basmati and other Asian rice variety groups [6, 7]. Recently, a study
629 suggested that *circum*-basmati rice (called 'aromatic' in that study) was a product of
630 hybridization between the *circum*-aus and japonica rice variety groups [17]. This inference was

631 based on observations of phylogenetic relationships across genomic regions that showed
632 evidence of domestication-related selective sweeps. These regions mostly grouped *circum*-
633 basmati with japonica or *circum*-aus. In addition, chloroplast haplotype analysis indicated that
634 most *circum*-basmati varieties carried a chloroplast derived from a wild rice most closely related
635 to *circum*-aus landraces [103]. Our evolutionary analysis of *circum*-basmati rice genomes
636 generally supported this view. Although our results suggest that *circum*-basmati had its origins
637 primarily in japonica, we also find significant evidence of gene flow originating from *circum*-
638 aus, which we detected both in comparative genomic and population genomic analyses.
639 Demographic modeling indicated a period of isolation among *circum*-aus, *circum*-basmati, and
640 japonica, with gene flow occurring only after lineage splitting of each group. Here, our model is
641 consistent with the current view that gene flow is a key evolutionary process associated with the
642 diversification of rice [10, 12–14, 16, 104, 105].

643 Interestingly, we found that chromosome 10 of *circum*-basmati had an evolutionary
644 history that differed significantly from that of other chromosomes. Specifically, compared to
645 japonica, this chromosome had the highest proportion of presence/absence variation, and shared
646 more alleles with *circum*-aus. Based on this result, we hypothesize that this is largely due to
647 higher levels of introgression from *circum*-aus into chromosome 10 compared to other
648 chromosomes. Such a deviation of evolutionary patterns on a single chromosome has been
649 observed in the *Aquilegia* genus [106], but to our knowledge has not been observed elsewhere.
650 Why this occurred is unclear at present, but it may be that selection has driven a higher
651 proportion of *circum*-aus alleles into chromosome 10. Future work will be necessary to clarify
652 the consequence of this higher level of admixture on chromosome 10.

653 Very little is known about population genomic diversity within *circum*-basmati. Our
654 analysis suggests the existence of at least three genetic groups within this variety group, and
655 these groups showed geographic structuring. Several varieties from Group 1 (Bhutan/Nepal) and
656 Group 3 (Iran/Pakistan) had population genomic signatures consistent with an admixed
657 population, while Group 2 (India/Bangladesh/Myanmar) was genetically more distinct from the
658 other two subpopulations. In addition, the geographic location of the India/Bangladesh/Myanmar
659 group largely overlaps the region where *circum*-aus varieties were historically grown [107, 108].
660 Given the extensive history of admixture that *circum*-basmati rices have with *circum*-aus, the
661 India/Bangladesh/Myanmar group may have been influenced particularly strongly by gene flow
662 from *circum*-aus. How these three genetic subpopulations were established may require a deeper
663 sampling with in-depth analysis, but the geographically structured genomic variation shows that
664 the diversity of *circum*-basmati has clearly been underappreciated. In addition, the Basmati 334
665 and Dom Sufid varieties, for which we generated genome assemblies in this study, both belong to
666 the Iran/Pakistan genetic group. Thus, our study still leaves a gap in our knowledge of genomic
667 variation in the Bhutan/Nepal and India/Bangladesh/Myanmar genetic groups, and varieties in
668 these groups would be obvious next targets for generating additional genome assemblies.
669

670 **CONCLUSIONS**

671 In conclusion, our study shows that generating high-quality plant genome assemblies is
672 feasible with relatively modest amounts of resources and data. Using nanopore sequencing, we
673 were able to produce contiguous, chromosome-level genome assemblies for cultivars in a rice
674 variety group that contains economically and culturally important varieties. Our reference
675 genome sequences have the potential to be important genomic resources for identifying single

676 nucleotide polymorphisms and larger structural variations that are unique to *circum*-basmati rice.
677 Analyzing *de novo* genome assemblies for a larger sample of Asian rice will be important for
678 uncovering and studying hidden population genomic variation too complex to study with only
679 short-read sequencing technology.
680
681 **MATERIALS AND METHODS**
682 **Plant material.** Basmati 334 (IRGC 27819; GeneSys passport:
683 https://purl.org/germplasm/id/23601903-f8c3-4642-a7fc-516a5bc154f7) is a basmati (*sensu*
684 *stricto*) landrace from Pakistan and was originally donated to the International Rice Research
685 Institute (IRRI) by the Agricultural Research Council (ARC) in Karachi (donor accession ID:
686 PAK. SR. NO. 39). Dom Sufid (IRGC 117265; GeneSys passport:
687 https://purl.org/germplasm/id/fb861458-09de-46c4-b9ca-f5c439822919) is a sadri landrace from
688 Iran. Seeds from accessions IRGC 27819 and IRGC 117265 were obtained from the IRRI seed
689 bank, surface-sterilized with bleach, and germinated in the dark on a wet paper towel for four
690 days. Seedlings were transplanted individually in pots containing continuously wet soil in a
691 greenhouse at New York University's Center for Genomics and Systems Biology and cultivated
692 under a 12h day-12h night photoperiod at 30°C. Plants were kept in the dark in a growth cabinet
693 under the same climatic conditions for four days prior to tissue harvesting. Continuous darkness
694 induced chloroplast degradation, which diminishes the amount of chloroplast DNA that would
695 otherwise end up in the DNA extracted from the leaves.
696
697 **DNA extractions.** Thirty-six 100-mg samples (3.6 g total) of leaf tissue from a total of 10 one-
698 month-old plants were flash-frozen at harvest for each accession and stored at -80ºC. DNA

699 extractions were performed by isolating the cell nuclei and gently lysing the nuclei to extract
700 intact DNA molecules [109]. Yields ranged between 140ng/ul and 150ng/ul.
701
702 **Library preparation and nanopore sequencing.** Genomic DNA was visualized on an agarose
703 gel to determine shearing. DNA was size-selected using BluePippin BLF7510 cassette (Sage
704 Science) and high-pass mode (>20 kb) and prepared using Oxford Nanopore Technologies'
705 standard ligation sequencing kit SQK-LSK109. FLO-MIN106 (R9.4) flowcells were used for
706 sequencing on the GridION X5 platform.
707
708 **Library preparation and Illumina sequencing.** Extracted genomic DNA was prepared for
709 short-read sequencing using the Illumina Nextera DNA Library Preparation Kit. Sequencing was
710 done on the Illumina HiSeq 2500 – HighOutput Mode v3 with 2×100 bp read configuration, at
711 the New York University Genomics Core Facility.
712
713 **Genome assembly, polishing, and scaffolding.** After completion of sequencing, the raw signal
714 intensity data was used for base calling using *flip flop* (version 2.3.5) from Oxford Nanopore
715 Technologies. Reads with a mean qscore (quality) greater than 8 and a read length greater than 8
716 kb were used, and trimmed for adaptor sequences using *Porechop*
717 (https://github.com/rrwick/Porechop). Raw nanopore sequencing reads were corrected using the
718 program *Canu* [110], and then assembled with the genome assembler *Flye* [111].
719 The initial draft assemblies were polished for three rounds using the raw nanopore reads
720 with *Racon* ver. 1.2.1 [112], and one round with *Medaka*
721 (https://github.com/nanoporetech/medaka) from Oxford Nanopore Technologies. Afterwards,

722 reads from Illunima sequencing were used by *bwa-mem* [113] to align to the draft genome
723 assemblies. The alignment files were then used by *Pilon* ver. 1.22 [114] for three rounds of
724 polishing.

725 Contigs were scaffolded using a reference genome-guided scaffolding approach
726 implemented in *RaGOO* [56]. Using the Nipponbare genome as a reference, we aligned the
727 *circum*-basmati genomes using *Minimap2* [115]. *RaGOO* was then used to order the assembly
728 contigs. Space between contigs was artificially filled in with 100 'N' blocks.

729 Genome assembly statistics were calculated using the *bbmap stats.sh* script from the
730 *BBTools* suite (https://jgi.doe.gov/data-and-tools/bbtools/). Completeness of the genome
731 assemblies was evaluated using *BUSCO* ver. 2.0 [116]. Synteny between the *circum*-basmati
732 genomes and the Nipponbare genome was visualized using *D-GENIES* [117]. Genome-wide
733 dotplot from *D-GENIES* indicated the initial genome assembly of Dom Sufid had an evidence of
734 a large chromosomal fusion between the ends of chromosome 4 and 10. Closer examination of
735 this contig (named contig_28 of Dom Sufid) showed the break point overlapped the telomeric
736 repeat sequence, indicating there had been a misassembly between the ends of chromosome 4
737 and 10. Hence, contig_28 was broken up into two so that each contig represented the respective
738 chromosome of origin, and were then subsequently scaffolded using *RaGOO*.

739 Inversions that were observed in the dot plot were computationally verified
740 independently using raw nanopore reads. The long read-aware aligner *ngmlr* [55] was used to
741 align the nanopore reads to the Nipponbare genome, after which the long read-aware structural
742 variation caller *sniffles* [55] was used to call and detect inversions.

743 The number of sites aligning to the Nipponbare genome was determined using the
744 *Mummer4* package [118]. Alignment delta files were analyzed with the *dnadiff* suite from the

745 *Mummer4* package to calculate the number of aligned sites, and the number of differences
746 between the Nipponbare genome and the *circum*-basmati genomes.
747
748 **Gene annotation and analysis.** Gene annotation was conducted using the *MAKER* program [52,
749 53]. An in-depth description of running *MAKER* can be found on the website:
750 https://gist.github.com/darencard/bb1001ac1532dd4225b030cf0cd61ce2. We used published
751 *Oryza* genic sequences as evidence for the gene modeling process. We downloaded the
752 Nipponbare cDNA sequences from RAP-DB (https://rapdb.dna.affrc.go.jp/) to supply as EST
753 evidence, while the protein sequences from the 13 *Oryza* species project [37] were used as
754 protein evidence for the *MAKER* pipeline. Repetitive regions identified from the repeat analysis
755 were used to mask out the repeat regions for this analysis. After a first round of running *MAKER*
756 the predicted genes were used by *SNAP* [119] and *Augustus* [120] to create a training dataset of
757 gene models, which was then used for a second round of *MAKER* gene annotation.
758 Orthology between the genes from different rice genomes was determined with
759 *Orthofinder* ver. 1.1.9 [59]. Ortholog statuses were visualized with the *UpSetR* package [121].
760 Gene ontology for the orthogroups that are missing specifically in the *circum*-basmati
761 were examined by using the japonica Nipponbare gene, and conducting a gene ontology
762 enrichment analysis on *agriGO* v2.0 [122]. Gene ontology enrichment analysis for the *circum*-
763 basmati specific orthogroups was conducted first by predicting the function and gene ontology of
764 each *circum*-basmati genome gene model using the eggnog pipeline [123]. We required an
765 ontology to have more than 10 genes as a member for further consideration, and enrichment was
766 tested through a hypergeometric test using the *GOstat* package [124].
767

**Repetitive DNA annotation.** The repeat content of each genome assembly was determined using *Repeatmasker* ver. 4.0.5 (http://www.repeatmasker.org/RMDownload.html). We used the *Oryza*-specific repeat sequences that were identified from Choi et al. [14] (DOI: 10.5061/dryad.7cr0q), who had used *Repeatmodeler* ver. 1.0.8 (http://www.repeatmasker.org/RepeatModeler.html) to *de novo*-annotate repetitive elements across wild and domesticated *Oryza* genomes [37].

LTR retrotransposons were annotated using the program *LTRharvest* [125] with parameters adapted from [126]. LTR retrotransposons were classified into superfamilies [76] using the program *RepeatClassifier* from the *RepeatModeler* suite. Annotated LTR retrotransposons were further classified into specific families using the 242 consensus sequences of LTR-RTs from the RetrOryza database [83]. We used *blastn* [127] to search the RetrOryza sequences, and each of our candidate LTR retrotransposons was identified using the "80-80-80" rule [76]: two TEs belong to the same family if they were 80% identical over at least 80 bp and 80% of their length.

Insertion times for the LTR retrotransposons were estimated using the DNA divergence between pairs of LTR sequences [75]. The L-INS-I algorithm in the alignment program *MAFFT* ver. 7.154b [128] was used to align the LTR sequences. *PAML* ver. 4.8 [129] was used to estimate the DNA divergence between the LTR sequences with the Kimura-2-parameter base substitution model [130]. DNA divergence was converted to divergence time (i.e. time since the insertion of a LTR retrotransposon) approximating a base substitution rate of $1.3\times10^{-8}$ [131], which is two times higher than the synonymous site substitution rate.

790 **Presence/absence variation detection.** PAVs between the Nipponbare genome and the *circum*-
791 Basmati assemblies were detected using the *Assemblytics* suites [60]. Initially, the Nipponbare
792 genome was used as the reference to align the *circum*-basmati assemblies using the program
793 *Minimap2*. The resulting SAM files were converted to files in delta format using the
794 *sam2delta.py* script from the *RaGOO* suite. The delta files were then uploaded onto the online
795 *Assemblytics* analysis pipeline (http://assemblytics.com/). Repetitive regions would cause
796 multiple regions in the Nipponbare or *circum*-basmati genomes to align to one another, and in
797 that case *Assemblytics* would call the same region as a PAV multiple times. Hence, any PAV
798 regions that overlapped for at least 70% of their genomic coordinates were collapsed to a single
799 region.

800 The combination of *ngmlr* and *sniffles* was also used to detect the PAVs that differed
801 between the Nipponbare genome and the raw nanopore reads for the *circum*-basmati rices.
802 Because *Assemblytics* only detects PAVs in the range of 50 bp to 100,000 bp, we used this
803 window as a size limit to filter out the PAVs called by *sniffles*. Only PAVs supported by more
804 than 5 reads by *sniffles* were analyzed.

805 *Assemblytics* and sniffles call the breakpoints of PAVs differently. *Assemblytics* calls a
806 single-best breakpoint based on the genome alignment, while *sniffles* calls a breakpoint across a
807 predicted interval. To find overlapping PAVs between *Assemblytics* and *sniffles* we added 500 bp
808 upstream and downstream of the *Assemblytics*-predicted breakpoint positions.
809
810 **Detecting gene deletions across the *circum*-basmati population.** Genome-wide deletion
811 frequencies of each gene were estimated using the 78-variety *circum*-basmati population
812 genomic dataset. For each of the 78 varieties, raw sequencing reads were aligned to the *circum*-

basmati and Nipponbare genomes using *bwa-mem*. Genome coverage per site was calculated using *bedtools genomecov* [132]. For each variety the average read coverage was calculated for each gene, and a gene was designated as deleted if its average coverage was less than 0.05×.

**Whole-genome alignment of *Oryza* genomes assembled *de novo*.** Several genomes from published studies that were assembled *de novo* were analyzed. These include domesticated Asian rice genomes from the japonica variety group cv. Nipponbare [33]; the indica variety group cvs. 93-11 [32], IR8 [37], IR64 [38], MH63 [40], R498 [41], and ZS97 [40]; the *circum*-aus variety group cvs. DJ123 [38], Kasalath [39], and N22 [37]; and the *circum*-basmati variety group cv. GP295-1 [42]. Three genomes from wild rice species were also analyzed; these were *O. barthii* [35], *O. nivara* [37], and *O. rufipogon* [37].

Alignment of the genomes assembled *de novo* was conducted using the approach outlined in Haudry *et al.* [133], and the alignment has been used in another rice comparative genomic study [14]. Briefly, this involved using the Nipponbare genome as the reference for aligning all other genome assemblies. Alignment between japonica and a query genome was conducted using *LASTZ* ver. 1.03.73 [134], and the alignment blocks were chained together using the UCSC Kent utilities [135]. For japonica genomic regions with multiple chains, the chain with the highest alignment score was chosen as the single-most orthologous region. This analyzes only one of the multiple regions that are potentially paralogous between the japonica and query genomes, but this was not expected to affect the downstream phylogenomic analysis of determining the origin and evolution of the *circum*-basmati rice variety group. All pairwise genome alignments between the japonica and query genomes were combined into a multi-genome alignment using *MULTIZ* [136].

836

837 **Phylogenomic analysis.** The multi-genome alignment was used to reconstruct the phylogenetic
838 relationships between the domesticated and wild rices. Four-fold degenerate sites based on the
839 gene model of the reference japonica genome were extracted using the *msa_view* program from
840 the *phast* package ver. 1.4 [137]. The four-fold degenerate sites were used by *RAxML* ver. 8.2.5
841 [138] to build a maximum likelihood-based tree, using a general time-reversible DNA
842 substitution model with gamma-distributed rate variation.

843 To investigate the genome-wide landscape of introgression and incomplete lineage
844 sorting we examined the phylogenetic topologies of each gene [139]. For a three-species
845 phylogeny using *O. barthii* as an outgroup there are three possible topologies. For each gene,
846 topology-testing methods [140] can be used to determine which topology significantly fits the
847 gene of interest [14]. *RAxML*-estimated site-likelihood values were calculated for each gene and
848 the significant topology was determined using the Approximately Unbiased (AU) test [86] from
849 the program *CONSEL* v. 0.20 [141]. Genes with AU test results with a likelihood difference of
850 zero were omitted and the topology with an AU test support of greater than 0.95 was selected.

851

852 **Testing for evidence of admixture.** Evidence of admixture between variety groups was detected
853 using the ABBA-BABA test D-statistics [87, 88]. In a rooted three-taxon phylogeny [i.e.
854 "((P1,P2),P3),O" where P1, P2, and P3 are the variety groups of interest and O is outgroup *O.*
855 *barthii*], admixture can be inferred from the combination of ancestral ("A") and derived ("B")
856 allelic states of each individual. The ABBA conformation arises when variety groups P2 and P3
857 share derived alleles, while the BABA conformation is found when P1 and P3 share derived
858 alleles. The difference in the frequency of the ABBA and BABA conformations is measured by

859 the D-statistics, where significantly positive D-statistics indicate admixture between the P2 and
860 P3 variety groups, and significantly negative D-statistics indicate admixture between the P1 and
861 P3 variety groups. The genome was divided into 100,000-bp bins for jackknife resampling and
862 calculation of the standard errors. The significance of the D-statistics was calculated using the Z-
863 test, and D-statistics with Z-scores greater than $|3.9|$ ($p < 0.0001$) were considered significant.
864
865 **Population genomic analysis.** We downloaded FASTQ files from the 3K Rice Genome Project
866 [7] for rice varieties that were determined to be *circum*-basmati varieties in that project. An
867 additional 8 *circum*-basmati varieties were sequenced on the Illumina sequencing platform as
868 part of this study. The raw reads were aligned to the scaffolded Basmati 334 genome using the
869 program *bwa-mem.* PCR duplicates were determined computationally and removed using the
870 program *picard* version 2.9.0 (http://broadinstitute.github.io/picard/). Genotype calls for each site
871 were conducted using the *GATK HaplotypeCaller* engine using the option `-ERC GVCF`. The
872 output files were in the genomic variant call format (gVCF), and the gVCFs from each variety
873 were merged using the *GATK GenotypeGVCFs* engine.
874 SNP and INDEL variants from the population variant file were filtered independently
875 using the *GATK* bestpractice hard filter pipeline [142]. SNP variants within 5 bps of an INDEL
876 variant were filtered. *Vcftools* version 0.1.15 [143] was used to filter sites for which genotypes
877 were not called for more than 20% of the varieties Because domesticated rice is an inbreeding
878 species we also implemented a heterozygosity filter by filtering out sites that had a heterozygote
879 genotype in more than 5% of the samples using the program *vcffilterjdk.jar* from the *jvarkit* suite
880 (https://figshare.com/articles/JVarkit_java_based_utilities_for_Bioinformatics/1425030).
881 Missing genotypes were imputed and phased using *Beagle* version 4.1 [144].

To examine the within-*circum*-basmati variety group population structure we first randomly pruned the sites by sampling a polymorphic site every 200,000 bp using *plink* [145]. *Plink* was also used to conduct a principal component analysis. Ancestry proportions of each sample were estimated using *fastSTRUCTURE* [91]. A neighbor-joining tree was built by calculating the pairwise genetic distances between samples using the Kronecker delta function-based equation [146]. From the genetic distance matrix a neighbor-joining tree was built using the program *FastME* [147].

**Evolutionary relationships among the *circum*-basmati, *circum*-aus, and japonica populations.** To investigate the evolutionary origins of the *circum*-basmati population, we focused on the landrace varieties that had been sequenced with a genome-wide coverage of greater than 14×. The population data for the *circum*-aus and japonica populations were obtained from the 3K Rice Genome Project [7], from which we also analyzed only the landrace varieties that had been sequenced with a genome-wide coverage greater than 14×. For an outgroup, we obtained *O. barthii* sequencing data from previous studies [35, 148], and focused on the samples that were not likely to be feralized rices [148]. The Illumina reads were aligned to the scaffolded Basmati 334 genome and SNPs were called and filtered according to the procedure outlined in the "Population genomic analysis" section.

We examined the genome-wide local topological relationship using *twisst* [89]. Initially, a sliding window analysis was conducted to estimate the local phylogenetic trees in windows with a size of 100 or 500 polymorphic sites using *RAxML* with the GTRCAT substitution model. The script *raxml_sliding_windows.py* from the *genomics_general* package by Simon Martin

(https://github.com/simonhmartin/genomics_general/tree/master/phylo) was used. The 'complete' option of *twisst* was used to calculate the exact weighting of each local window.

**□a□i demographic model.** The demography model underlying the evolution of *circum*-basmati rice was tested using the diffusion approximation method of *δaδi* [90]. A visual representation of the 13 demographic models that were examined can be seen in Supplementary Figure S6. The population group and genotype calls used in the twisst analysis were also used to calculate the site allele frequencies. Polymorphic sites were polarized using the *O. barthii* reference genome. We used a previously published approach [148], which generates an *O. barthii*-ized basmati genome sequence. This was accomplished using the Basmati 334 reference genome to align the *O. barthii* genome. For every basmati genome sequence position was then changed into the aligned *O. barthii* sequence. Gaps, missing sequence, and repetitive DNA region were denoted as 'N'.

We optimized the model parameter estimates using the Nelder-Mead method and randomly perturbed the parameter values for four rounds. Parameter values were perturbed for three-fold, two-fold, two-fold, and one-fold in each subsequent round, while the perturbation was conducted for 10, 20, 30, and 40 replicates in each subsequent round. In each round parameter values from the best likelihood model of the previous round were used as the starting parameter values for the next round. Parameter values from the round with the highest likelihood were chosen to parameterize each demographic model. Akaike Information Criteria (AIC) values were used to compare demography models. The demography model with the lowest AIC was chosen as the best-fitting model.

927 **Agronomic trait measurements.** Data on geolocation of collection as well as on seed
928 dimensions and seed weight for each of the *circum*-basmati landrace varieties included in this
929 study were obtained from passport data included in the online platform Genesys
930 (https://www.genesys-pgr.org/welcome).
931
932 **DECLARATIONS**
933 **Ethics approval and consent to participate.** Not applicable.
934
935 **Consent for publication.** Not applicable.
936
937 **Availability of data and materials.** Raw nanopore sequencing FAST5 files generated from this
938 study are available at the European Nucleotide Archive under bioproject ID PRJEB28274
939 (ERX3327648-ERX3327652) for Basmati 334 and PRJEB32431 (ERX3334790-ERX3334793)
940 for Dom Sufid. Associated FASTQ files are available under ERX3498039-ERX3498043 for
941 Basmati 334 and ERX3498024-ERX3498027 for Dom Sufid. Illumina sequencing generated
942 from this study can be found under bioproject ID PRJNA422249 and PRJNA557122. A genome
943 browser for both genome assemblies can be found at http://purugganan-
944 genomebrowser.bio.nyu.edu/cgi-bin/hgTracks?db=Basmati334 for Basmati 334, and
945 http://purugganan-genomebrowser.bio.nyu.edu/cgi-bin/hgTracks?db=DomSufid for Dom Sufid.
946 All data including the assembly, annotation, genome alignment, and population VCFs generated
947 from this study can be found at https://doi.org/10.5281/zenodo.3355330.
948

**Competing interests.** XD, PR, EDH, and SJ are employees of Oxford Nanopore Technologies and are shareholders and/or share option holders.

**Funding.** This work was supported by grants from the Gordon and Betty Moore Foundation through Grant GBMF2550.06 to S.C.G., and from the National Science Foundation Plant Genome Research Program (IOS-1546218), the Zegar Family Foundation (A16-0051) and the NYU Abu Dhabi Research Institute (G1205) to M.D.P. The funding body had no role in the design of the study and collection, analysis, and interpretation of data and in writing the manuscript.

**Authors' contributions.** JYC, SCG, SZ, and MDP conceived the project and its components. JYC, SCG, and SZ prepared the sample material for sequencing. XD, PR, EDH, and SJ conducted the genome sequencing and assembling. JYC, ZNL, and SCG performed the data analysis. JYC and ZNL prepared the figures and tables. JYC and MDP wrote the manuscript with help from ZNL and SCG.

**Acknowledgements.** We thank Katherine Dorph for assistance with growing and maintaining the plants, and Adrian Platts for computational support. We thank Rod Wing, David Kudrna, and Jayson Talag from Arizona Genomics Institute with the high-molecular weight DNA extraction. We thank the New York University Genomics Core Facility for sequencing support and the New York University High Performance Computing for supplying the computational resources.

**REFERENCES**

1. Gnanamanickam SS. Rice and Its Importance to Human Life. In: Biological Control of Rice Diseases. Dordrecht: Springer Netherlands; 2009. p. 1–11. doi:10.1007/978-90-481-2465-7_1.

2. Matsuo T, Futsuhara Y, Kikuchi F, Yamaguchi H. Science of the Rice Plant. Tokyo: Food and Agriculture Policy Research Center; 1997.

3. Gross BL, Zhao Z. Archaeological and genetic insights into the origins of domesticated rice. Proc Natl Acad Sci USA. 2014;111:6190–7.

4. Nadir S, Khan S, Zhu Q, Henry D, Wei L, Lee DS, et al. An overview on reproductive isolation in Oryza sativa complex. AoB Plants. 2018;10:ply060.

5. Fuller DQ, Sato Y-I, Castillo C, Qin L, Weisskopf AR, Kingwell-Banham EJ, et al. Consilience of genetics and archaeobotany in the entangled history of rice. Archaeol Anthropol Sci. 2010;2:115–31.

6. Garris AJ, Tai TH, Coburn J, Kresovich S, McCouch S. Genetic structure and diversity in Oryza sativa L. Genetics. 2005;169:1631–8.

7. Wang W, Mauleon R, Hu Z, Chebotarov D, Tai S, Wu Z, et al. Genomic variation in 3,010 diverse accessions of Asian cultivated rice. Nature. 2018;557:43–9.

8. Glaszmann JC. Isozymes and classification of Asian rice varieties. Theoret Appl Genetics. 1987;74:21–30.

9. He Z, Zhai W, Wen H, Tang T, Wang Y, Lu X, et al. Two evolutionary histories in the genome of rice: the roles of domestication genes. PLoS Genet. 2011;7:e1002100.

10. Fuller DQ. Pathways to Asian Civilizations: Tracing the Origins and Spread of Rice and Rice Cultures. Rice. 2012;4:78–92.

11. Meyer RS, Purugganan MD. Evolution of crop species: genetics of domestication and diversification. Nat Rev Genet. 2013;14:840–52.

12. Huang X, Han B. Rice domestication occurred through single origin and multiple introgressions. Nat Plants. 2015;2:15207.

13. Castillo CC, Tanaka K, Sato Y-I, Ishikawa R, Bellina B, Higham C, et al. Archaeogenetic study of prehistoric rice remains from Thailand and India: evidence of early japonica in South and Southeast Asia. Archaeological and Anthropological Sciences. 2016;8:523–43.

14. Choi JY, Platts AE, Fuller DQ, Hsing Y-I, Wing RA, Purugganan MD. The rice paradox: Multiple origins but single domestication in Asian rice. Molecular Biology and Evolution. 2017;34:969–79.

15. Choi JY, Purugganan MD. Multiple Origin but Single Domestication Led to Oryza sativa. G3: Genes, Genomes, Genetics. 2018;8:797–803.

16. Huang X, Kurata N, Wei X, Wang Z-X, Wang A, Zhao Q, et al. A map of rice genome variation reveals the origin of cultivated rice. Nature. 2012;490:497–501.

17. Civáň P, Craig H, Cox CJ, Brown TA. Three geographically separate domestications of Asian rice. Nat Plants. 2015;1:15164.

18. Wang ZY, Zheng FQ, Shen GZ, Gao JP, Snustad DP, Li MG, et al. The amylose content in rice endosperm is related to the post-transcriptional regulation of the waxy gene. Plant J. 1995;7:613–22.

19. Sweeney MT, Thomson MJ, Pfeil BE, McCouch S. Caught red-handed: Rc encodes a basic helix-loop-helix protein conditioning red pericarp in rice. Plant Cell. 2006;18:283–94.

20. Konishi S, Izawa T, Lin SY, Ebana K, Fukuta Y, Sasaki T, et al. An SNP Caused Loss of Seed Shattering During Rice Domestication. Science. 2006;312:1392–6.

21. Kovach MJ, Calingacion MN, Fitzgerald MA, McCouch SR. The origin and evolution of fragrance in rice (Oryza sativa L.). Proceedings of the National Academy of Sciences of the United States of America. 2009;106:14444–9.

22. Xu K, Xu X, Fukao T, Canlas P, Maghirang-Rodriguez R, Heuer S, et al. Sub1A is an ethylene-response-factor-like gene that confers submergence tolerance to rice. Nature. 2006;442:705–8.

23. Bin Rahman ANMR, Zhang J. Preferential Geographic Distribution Pattern of Abiotic Stress Tolerant Rice. Rice. 2018;11:10.

24. Singh R, Singh U, Khush G, editors. Aromatic rices. Oxford & IBH Publishing Co Pvt Ltd; 2000.

25. Bradbury LMT, Gillies SA, Brushett DJ, Waters DLE, Henry RJ. Inactivation of an aminoaldehyde dehydrogenase is responsible for fragrance in rice. Plant Mol Biol. 2008;68:439–49.

26. Chen S, Yang Y, Shi W, Ji Q, He F, Zhang Z, et al. Badh2, Encoding Betaine Aldehyde Dehydrogenase, Inhibits the Biosynthesis of 2-Acetyl-1-Pyrroline, a Major Component in Rice Fragrance. Plant Cell. 2008;20:1850–61.

27. Zhao K, Tung C-W, Eizenga GC, Wright MH, Ali ML, Price AH, et al. Genome-wide association mapping reveals a rich genetic architecture of complex traits in Oryza sativa. Nature Communications. 2011;2:467.

28. Heather JM, Chain B. The sequence of sequencers: The history of sequencing DNA. Genomics. 2016;107:1–8.

29. Michael TP, VanBuren R. Progress, challenges and the future of crop genomes. Current Opinion in Plant Biology. 2015;24:71–81.

30. Jiao W-B, Schneeberger K. The impact of third generation genomic technologies on plant genome assembly. Current Opinion in Plant Biology. 2017;36:64–70.

31. Li C, Lin F, An D, Wang W, Huang R. Genome Sequencing and Assembly by Long Reads in Plants. Genes. 2017;9. doi:10.3390/genes9010006.

32. Yu J, Hu S, Wang J, Wong GK-S, Li S, Liu B, et al. A draft sequence of the rice genome (Oryza sativa L. ssp. indica). Science. 2002;296:79–92.

33. International Rice Genome Sequencing Project. The map-based sequence of the rice genome. Nature. 2005;436:793–800.

34. Chen J, Huang Q, Gao D, Wang J, Lang Y, Liu T, et al. Whole-genome sequencing of Oryza brachyantha reveals mechanisms underlying Oryza genome evolution. Nat Commun. 2013;4:1595.

35. Wang M, Yu Y, Haberer G, Marri PR, Fan C, Goicoechea JL, et al. The genome sequence of African rice (Oryza glaberrima) and evidence for independent domestication. Nat Genet. 2014;46:982–8.

36. Zhang Y, Zhang S, Liu H, Fu B, Li L, Xie M, et al. Genome and Comparative Transcriptomics of African Wild Rice Oryza longistaminata Provide Insights into Molecular Mechanism of Rhizomatousness and Self-Incompatibility. Molecular Plant. 2015;8:1683–6.

37. Stein JC, Yu Y, Copetti D, Zwickl DJ, Zhang L, Zhang C, et al. Genomes of 13 domesticated and wild rice relatives highlight genetic conservation, turnover and innovation across the genus Oryza. Nature Genetics. 2018;50:285.

38. Schatz MC, Maron LG, Stein JC, Wences A, Gurtowski J, Biggers E, et al. Whole genome de novo assemblies of three divergent strains of rice, Oryza sativa , document novel gene space of aus and indica. Genome Biology. 2014;15:506.

39. Sakai H, Kanamori H, Arai-Kichise Y, Shibata-Hatta M, Ebana K, Oono Y, et al. Construction of Pseudomolecule Sequences of the aus Rice Cultivar Kasalath for Comparative Genomics of Asian Cultivated Rice. DNA Research. 2014;21:397–405.

40. Zhang J, Chen L-L, Xing F, Kudrna DA, Yao W, Copetti D, et al. Extensive sequence divergence between the reference genomes of two elite indica rice varieties Zhenshan 97 and Minghui 63. Proceedings of the National Academy of Sciences of the United States of America. 2016;113:E5163-71.

41. Du H, Yu Y, Ma Y, Gao Q, Cao Y, Chen Z, et al. Sequencing and de novo assembly of a near complete indica rice genome. Nature Communications. 2017;8:15324.

42. Zhao Q, Feng Q, Lu H, Li Y, Wang A, Tian Q, et al. Pan-genome analysis highlights the extent of genomic variation in cultivated and wild rice. Nature Genetics. 2018;50:278–84.

1073 43. Jain S, Jain RK, McCouch SR. Genetic analysis of Indian aromatic and quality rice (Oryza
1074 sativa L.) germplasm using panels of fluorescently-labeled microsatellite markers. Theoretical
1075 and Applied Genetics. 2004;109:965–77.

1076 44. Vikram P, Swamy BPM, Dixit S, Ahmed H, Cruz MTS, Singh AK, et al. Bulk segregant
1077 analysis: "An effective approach for mapping consistent-effect drought grain yield QTLs in
1078 rice." Field Crops Research. 2012;134:185–92.

1079 45. McNally KL, Childs KL, Bohnert R, Davidson RM, Zhao K, Ulat VJ, et al. Genomewide
1080 SNP variation reveals relationships among landraces and modern varieties of rice. Proceedings
1081 of the National Academy of Sciences. 2009;106:12273–8.

1082 46. McNally KL, Bruskiewich R, Mackill D, Buell CR, Leach JE, Leung H. Sequencing
1083 Multiple and Diverse Rice Varieties. Connecting Whole-Genome Variation with Phenotypes.
1084 Plant Physiology. 2006;141:26–31.

1085 47. Jain M, Olsen HE, Paten B, Akeson M. The Oxford Nanopore MinION: delivery of nanopore
1086 sequencing to the genomics community. Genome Biology. 2016;17:239.

1087 48. Chen S, Huang Z, Zeng L, Yang J, Liu Q, Zhu X. High-resolution mapping and gene
1088 prediction of Xanthomonas Oryzae pv. Oryzae resistance gene Xa7. Molecular Breeding.
1089 2008;22:433–41.

1090 49. Ullah I, Jamil S, Iqbal MZ, Shaheen HL, Hasni SM, Jabeen S, et al. Detection of bacterial
1091 blight resistance genes in basmati rice landraces. Genetics and Molecular Research.
1092 2012;11:1960–6.

1093 50. Sandhu N, Kumar A, Sandhu N, Kumar A. Bridging the Rice Yield Gaps under Drought:
1094 QTLs, Genes, and their Use in Breeding Programs. Agronomy. 2017;7:27.

1095 51. Henry A, Gowda VRP, Torres RO, McNally KL, Serraj R. Variation in root system
1096 architecture and drought response in rice (Oryza sativa): Phenotyping of the OryzaSNP panel in
1097 rainfed lowland fields. Field Crops Research. 2011;120:205–14.

1098 52. Cantarel BL, Korf I, Robb SMC, Parra G, Ross E, Moore B, et al. MAKER: An easy-to-use
1099 annotation pipeline designed for emerging model organism genomes. Genome Res.
1100 2008;18:188–96.

1101 53. Holt C, Yandell M. MAKER2: an annotation pipeline and genome-database management
1102 tool for second-generation genome projects. BMC Bioinformatics. 2011;12:491.

1103 54. Choi JY, Purugganan MD. Evolutionary epigenomics of retrotransposon-mediated
1104 methylation spreading in rice. Molecular Biology and Evolution. 2018;35:365–82.

1105 55. Sedlazeck FJ, Rescheneder P, Smolka M, Fang H, Nattestad M, von Haeseler A, et al.
1106 Accurate detection of complex structural variations using single-molecule sequencing. Nature
1107 Methods. 2018;15:461–8.

1108 56. Alonge M, Soyk S, Ramakrishnan S, Wang X, Goodwin S, Sedlazeck FJ, et al. Fast and
1109 accurate reference-guided scaffolding of draft genomes. bioRxiv. 2019;:519637.

1110 57. Kawahara Y, de la Bastide M, Hamilton JP, Kanamori H, McCombie WR, Ouyang S, et al.
1111 Improvement of the Oryza sativa Nipponbare reference genome using next generation sequence
1112 and optical map data. Rice. 2013;6:4.

1113 58. Sakai H, Lee SS, Tanaka T, Numa H, Kim J, Kawahara Y, et al. Rice Annotation Project
1114 Database (RAP-DB): An Integrative and Interactive Database for Rice Genomics. Plant and Cell
1115 Physiology. 2013;54:e6–e6.

1116 59. Emms DM, Kelly S. OrthoFinder: solving fundamental biases in whole genome comparisons
1117 dramatically improves orthogroup inference accuracy. Genome Biology. 2015;16:157.

1118 60. Nattestad M, Schatz MC. Assemblytics: a web analytics tool for the detection of variants
1119 from an assembly. Bioinformatics. 2016;32:3021–3.

1120 61. Fuentes RR, Chebotarov D, Duitama J, Smith S, Hoz JFD la, Mohiyuddin M, et al. Structural
1121 variants in 3000 rice genomes. Genome Res. 2019;29:870–80.

1122 62. Shomura A, Izawa T, Ebana K, Ebitani T, Kanegae H, Konishi S, et al. Deletion in a gene
1123 associated with grain size increased yields during rice domestication. Nature Genetics.
1124 2008;40:1023–8.

1125 63. Zhou Y, Zhu J, Li Z, Yi C, Liu J, Zhang H, et al. Deletion in a Quantitative Trait Gene qPE9-
1126 1 Associated With Panicle Erectness Improves Plant Architecture During Rice Domestication.
1127 Genetics. 2009;183:315–24.

1128 64. Lye ZN, Purugganan MD. Copy Number Variation in Domestication. Trends in Plant
1129 Science. 2019;24:352–65.

1130 65. Hu M, Lv S, Wu W, Fu Y, Liu F, Wang B, et al. The domestication of plant architecture in
1131 African rice. The Plant Journal. 2018;94:661–9.

1132 66. Wu Y, Zhao S, Li X, Zhang B, Jiang L, Tang Y, et al. Deletions linked to PROG1 gene
1133 participate in plant architecture domestication in Asian and African rice. Nature
1134 Communications. 2018;9:4157.

1135 67. Li B, Zhang Y, Li J, Yao G, Pan H, Hu G, et al. Fine Mapping of Two Additive Effect Genes
1136 for Awn Development in Rice (Oryza sativa L.). PLOS ONE. 2016;11:e0160792.

1137 68. Hua L, Wang DR, Tan L, Fu Y, Liu F, Xiao L, et al. LABA1, a Domestication Gene
1138 Associated with Long, Barbed Awns in Wild Rice. The Plant Cell. 2015;27:1875–88.

1139 69. Kumar A, Bennetzen JL. Plant Retrotransposons. Annual Review of Genetics. 1999;33:479–
1140 532.

1141 70. Zuccolo A, Sebastian A, Talag J, Yu Y, Kim H, Collura K, et al. Transposable element
1142 distribution, abundance and role in genome size variation in the genus Oryza. BMC Evol Biol.
1143 2007;7:152.

1144 71. Lerat E. Identifying repeats and transposable elements in sequenced genomes: how to find
1145 your way through the dense forest of programs. Heredity. 2010;104:520–33.

1146 72. Hoen DR, Hickey G, Bourque G, Casacuberta J, Cordaux R, Feschotte C, et al. A call for
1147 benchmarking transposable element annotation methods. Mobile DNA. 2015;6:13.

1148 73. Bennetzen JL. The contributions of retroelements to plant genome organization, function and
1149 evolution. Trends Microbiol. 1996;4:347–53.

1150 74. Voytas DF, Ausubel FM. A copia-like transposable element family in Arabidopsis thaliana.
1151 Nature. 1988;336:242–4.

1152 75. SanMiguel P, Gaut BS, Tikhonov A, Nakajima Y, Bennetzen JL. The paleontology of
1153 intergene retrotransposons of maize. Nature Genetics. 1998;20:43–5.

1154 76. Wicker T, Sabot F, Hua-Van A, Bennetzen JL, Capy P, Chalhoub B, et al. A unified
1155 classification system for eukaryotic transposable elements. Nature Reviews Genetics.
1156 2007;8:973–82.

1157 77. Vitte C, Panaud O, Quesneville H. LTR retrotransposons in rice (Oryza sativa, L.): recent
1158 burst amplifications followed by rapid DNA loss. BMC Genomics. 2007;8:218.

1159 78. Panaud O, Vitte C, Hivert J, Muzlak S, Talag J, Brar D, et al. Characterization of
1160 transposable elements in the genome of rice (Oryza sativa L.) using Representational Difference
1161 Analysis (RDA). Molecular genetics and genomics : MGG. 2002;268:113–21.

1162 79. McCarthy EM, Liu J, Lizhi G, McDonald JF. Long terminal repeat retrotransposons of Oryza
1163 sativa. Genome biology. 2002;3:RESEARCH0053.

1164 80. Carpentier M-C, Manfroi E, Wei F-J, Wu H-P, Lasserre E, Llauro C, et al.
1165 Retrotranspositional landscape of Asian rice revealed by 3000 genomes. Nat Commun. 2019;10.
1166 doi:10.1038/s41467-018-07974-5.

1167 81. Zhang Q-J, Gao L-Z. Rapid and Recent Evolution of LTR Retrotransposons Drives Rice
1168 Genome Evolution During the Speciation of AA- Genome Oryza Species. G3: Genes, Genomes,
1169 Genetics. 2017;:g3.116.037572.

1170 82. Kumekawa N, Ohtsubo H, Horiuchi T, Ohtsubo E. Identification and characterization of
1171 novel retrotransposons of the gypsy type in rice. Mol Gen Genet. 1999;260:593–602.

1172 83. Chaparro C, Guyot R, Zuccolo A, Piégu B, Panaud O. RetrOryza: a database of the rice
1173 LTR-retrotransposons. Nucleic acids research. 2007;35 Database issue:D66-70.

1174 84. Wang H, Vieira FG, Crawford JE, Chu C, Nielsen R. Asian wild rice is a hybrid swarm with
1175 extensive gene flow and feralization from domesticated rice. Genome research. 2017;27:1029–
1176 38.

1177 85. Li L-F, Li Y-L, Jia Y, Caicedo AL, Olsen KM. Signatures of adaptation in the weedy rice
1178 genome. Nature genetics. 2017;49:811–4.

1179 86. Shimodaira H. An approximately unbiased test of phylogenetic tree selection. Syst Biol.
1180 2002;51:492–508.

1181 87. Green RE, Krause J, Briggs AW, Maricic T, Stenzel U, Kircher M, et al. A draft sequence of
1182 the Neandertal genome. Science. 2010;328:710–22.

1183 88. Durand EY, Patterson N, Reich D, Slatkin M. Testing for Ancient Admixture between
1184 Closely Related Populations. Molecular Biology and Evolution. 2011;28:2239–52.

1185 89. Martin SH, Van Belleghem SM. Exploring Evolutionary Relationships Across the Genome
1186 Using Topology Weighting. Genetics. 2017;206:429–38.

1187 90. Gutenkunst RN, Hernandez RD, Williamson SH, Bustamante CD. Inferring the joint
1188 demographic history of multiple populations from multidimensional SNP frequency data. PLoS
1189 Genet. 2009;5:e1000695.

1190 91. Raj A, Stephens M, Pritchard JK. fastSTRUCTURE: variational inference of population
1191 structure in large SNP data sets. Genetics. 2014;197:573–89.

1192 92. Michael TP, Jupe F, Bemm F, Motley ST, Sandoval JP, Lanz C, et al. High contiguity
1193 Arabidopsis thaliana genome assembly with a single nanopore flow cell. Nature
1194 Communications. 2018;9:541.

1195 93. Schmidt MH, Vogel A, Denton AK, Istace B, Wormit A, van de Geest H, et al. De novo
1196 Assembly of a New Solanum pennellii Accession Using Nanopore Sequencing. The Plant cell.
1197 2017;:tpc.00521.2017.

1198 94. Belser C, Istace B, Denis E, Dubarry M, Baurens F-C, Falentin C, et al. Chromosome-scale
1199 assemblies of plant genomes using nanopore long reads and optical maps. Nature Plants.
1200 2018;4:879.

1201 95. Howe K, Wood JM. Using optical mapping data for the improvement of vertebrate genome
1202 assemblies. GigaScience. 2015;4:10.

1203 96. Goodwin S, McPherson JD, McCombie WR. Coming of age: ten years of next-generation
1204 sequencing technologies. Nature Reviews Genetics. 2016;17:333–51.

1205 97. Udall JA, Dawe RK. Is It Ordered Correctly? Validating Genome Assemblies by Optical
1206 Mapping. The Plant cell. 2018;30:7–14.

98. Sedlazeck FJ, Lee H, Darby CA, Schatz MC. Piercing the dark matter: bioinformatics of long-range sequencing and mapping. Nature Reviews Genetics. 2018;19:329–46.

99. Wendel JF, Jackson SA, Meyers BC, Wing RA. Evolution of plant genome architecture. Genome Biology. 2016;17:37.

100. vonHoldt BM, Takuno S, Gaut BS. Recent Retrotransposon Insertions Are Methylated and Phylogenetically Clustered in Japonica Rice (Oryza sativa spp. japonica). Molecular Biology and Evolution. 2012;29:3193–203.

101. Baucom RS, Estill JC, Leebens-Mack J, Bennetzen JL. Natural selection on gene function drives the evolution of LTR retrotransposon families in the rice genome. Genome Research. 2009;19:243–54.

102. Naito K, Zhang F, Tsukiyama T, Saito H, Hancock CN, Richardson AO, et al. Unexpected consequences of a sudden and massive transposon amplification on rice gene expression. Nature. 2009;461:1130–4.

103. Civáň P, Ali S, Batista-Navarro R, Drosou K, Ihejieto C, Chakraborty D, et al. Origin of the Aromatic Group of Cultivated Rice (Oryza sativa L.) Traced to the Indian Subcontinent. Genome Biol Evol. 2019;11:832–43.

104. Molina J, Sikora M, Garud N, Flowers JM, Rubinstein S, Reynolds A, et al. Molecular evidence for a single evolutionary origin of domesticated rice. Proc Natl Acad Sci USA. 2011;108:8351–6.

105. Fuller DQ. Finding Plant Domestication in the Indian Subcontinent. Current Anthropology. 2011;52:S347–62.

106. Filiault DL, Ballerini ES, Mandáková T, Aköz G, Derieg NJ, Schmutz J, et al. The Aquilegia genome provides insight into adaptive radiation and reveals an extraordinarily polymorphic chromosome with a unique history. eLife. 2018;7:e36426.

107. Liakat Ali M, McClung AM, Jia MH, Kimball JA, McCouch, Georgia CE. A Rice Diversity Panel Evaluated for Genetic and Agro-Morphological Diversity between Subpopulations and its Geographic Distribution. Crop Science. 2011;51:2021–35.

108. Travis AJ, Norton GJ, Datta S, Sarma R, Dasgupta T, Savio FL, et al. Assessing the genetic diversity of rice originating from Bangladesh, Assam and West Bengal. Rice (N Y). 2015;8:35.

109. Zhang H-B, Zhao X, Ding X, Paterson AH, Wing RA. Preparation of megabase-size DNA from plant nuclei. The Plant Journal. 1995;7:175–84.

110. Koren S, Walenz BP, Berlin K, Miller JR, Bergman NH, Phillippy AM. Canu: scalable and accurate long-read assembly via adaptive k-mer weighting and repeat separation. Genome research. 2017;27:722–36.

111. Kolmogorov M, Yuan J, Lin Y, Pevzner PA. Assembly of long, error-prone reads using repeat graphs. Nature Biotechnology. 2019;37:540.

112. Vaser R, Sović I, Nagarajan N, Šikić M. Fast and accurate de novo genome assembly from long uncorrected reads. Genome research. 2017;27:737–46.

113. Li H. Aligning sequence reads, clone sequences and assembly contigs with BWA-MEM. arXiv. 2013;:1303.3997v2.

114. Walker BJ, Abeel T, Shea T, Priest M, Abouelliel A, Sakthikumar S, et al. Pilon: An Integrated Tool for Comprehensive Microbial Variant Detection and Genome Assembly Improvement. PLoS ONE. 2014;9:e112963.

115. Li H. Minimap2: pairwise alignment for nucleotide sequences. Bioinformatics. 2018;34:3094–100.

116. Simão FA, Waterhouse RM, Ioannidis P, Kriventseva EV, Zdobnov EM. BUSCO: assessing genome assembly and annotation completeness with single-copy orthologs. Bioinformatics. 2015;31:3210–2.

117. Cabanettes F, Klopp C. D-GENIES: dot plot large genomes in an interactive, efficient and simple way. PeerJ. 2018;6. doi:10.7717/peerj.4958.

118. Marçais G, Delcher AL, Phillippy AM, Coston R, Salzberg SL, Zimin A. MUMmer4: A fast and versatile genome alignment system. PLOS Computational Biology. 2018;14:e1005944.

119. Korf I. Gene finding in novel genomes. BMC Bioinformatics. 2004;5:59.

120. Stanke M, Diekhans M, Baertsch R, Haussler D. Using native and syntenically mapped cDNA alignments to improve de novo gene finding. Bioinformatics. 2008;24:637–44.

121. Conway JR, Lex A, Gehlenborg N, Hancock J. UpSetR: an R package for the visualization of intersecting sets and their properties. Bioinformatics. 2017;33:2938–40.

122. Tian T, Liu Y, Yan H, You Q, Yi X, Du Z, et al. agriGO v2.0: a GO analysis toolkit for the agricultural community, 2017 update. Nucleic Acids Res. 2017;45 Web Server issue:W122–9.

123. Huerta-Cepas J, Forslund K, Coelho LP, Szklarczyk D, Jensen LJ, von Mering C, et al. Fast Genome-Wide Functional Annotation through Orthology Assignment by eggNOG-Mapper. Mol Biol Evol. 2017;34:2115–22.

124. Falcon S, Gentleman R. Using GOstats to test gene lists for GO term association. Bioinformatics. 2007;23:257–8.

125. Ellinghaus D, Kurtz S, Willhoeft U. LTRharvest, an efficient and flexible software for de novo detection of LTR retrotransposons. BMC bioinformatics. 2008;9:18.

126. Copetti D, Zhang J, El Baidouri M, Gao D, Wang J, Barghini E, et al. RiTE database: a resource database for genus-wide rice genomics and evolutionary biology. BMC Genomics. 2015;16:538.

127. Camacho C, Coulouris G, Avagyan V, Ma N, Papadopoulos J, Bealer K, et al. BLAST+: architecture and applications. BMC Bioinformatics. 2009;10:421.

128. Katoh K, Standley DM. MAFFT Multiple Sequence Alignment Software Version 7: Improvements in Performance and Usability. Molecular Biology and Evolution. 2013;30:772–80.

129. Yang Z. PAML 4: Phylogenetic Analysis by Maximum Likelihood. Molecular Biology and Evolution. 2007;24:1586–91.

130. Kimura M. A simple method for estimating evolutionary rates of base substitutions through comparative studies of nucleotide sequences. Journal of molecular evolution. 1980;16:111–20.

131. Ma J, Bennetzen JL. Rapid recent growth and divergence of rice nuclear genomes. Proc Natl Acad Sci USA. 2004;101:12404–10.

132. Quinlan AR, Hall IM. BEDTools: a flexible suite of utilities for comparing genomic features. Bioinformatics. 2010;26:841–2.

133. Haudry A, Platts AE, Vello E, Hoen DR, Leclercq M, Williamson RJ, et al. An atlas of over 90,000 conserved noncoding sequences provides insight into crucifer regulatory regions. Nat Genet. 2013;45:891–8.

134. Harris RS. Improved pairwise alignment of genomic dna. PhD Thesis, The Pennsylvania State University. 2007.

135. Kent WJ, Baertsch R, Hinrichs A, Miller W, Haussler D. Evolution's cauldron: duplication, deletion, and rearrangement in the mouse and human genomes. Proc Natl Acad Sci USA. 2003;100:11484–9.

136. Blanchette M, Kent WJ, Riemer C, Elnitski L, Smit AFA, Roskin KM, et al. Aligning multiple genomic sequences with the threaded blockset aligner. Genome Res. 2004;14:708–15.

137. Hubisz MJ, Pollard KS, Siepel A. PHAST and RPHAST: phylogenetic analysis with space/time models. Brief Bioinformatics. 2011;12:41–51.

138. Stamatakis A. RAxML version 8: a tool for phylogenetic analysis and post-analysis of large phylogenies. Bioinformatics. 2014;30:1312–3.

139. Martin SH, Jiggins CD. Interpreting the genomic landscape of introgression. Current Opinion in Genetics & Development. 2017;47:69–74.

140. Goldman N, Anderson JP, Rodrigo AG, Olmstead R. Likelihood-Based Tests of Topologies in Phylogenetics. Systematic Biology. 2000;49:652–70.

141. Shimodaira H, Hasegawa M. CONSEL: for assessing the confidence of phylogenetic tree selection. Bioinformatics. 2001;17:1246–7.

142. Van der Auwera GA, Carneiro MO, Hartl C, Poplin R, del Angel G, Levy-Moonshine A, et al. From FastQ Data to High-Confidence Variant Calls: The Genome Analysis Toolkit Best Practices Pipeline. In: Current Protocols in Bioinformatics. Hoboken, NJ, USA: John Wiley & Sons, Inc.; 2013. p. 11.10.1-11.10.33. doi:10.1002/0471250953.bi1110s43.

143. Danecek P, Auton A, Abecasis G, Albers CA, Banks E, DePristo MA, et al. The variant call format and VCFtools. Bioinformatics. 2011;27:2156–8.

144. Browning BL, Browning SR. Genotype Imputation with Millions of Reference Samples. The American Journal of Human Genetics. 2016;98:116–26.

145. Purcell S, Neale B, Todd-Brown K, Thomas L, Ferreira MAR, Bender D, et al. PLINK: A Tool Set for Whole-Genome Association and Population-Based Linkage Analyses. The American Journal of Human Genetics. 2007;81:559–75.

146. Freedman AH, Gronau I, Schweizer RM, Ortega-Del Vecchyo D, Han E, Silva PM, et al. Genome sequencing highlights the dynamic early history of dogs. PLoS Genet. 2014;10:e1004016.

147. Lefort V, Desper R, Gascuel O. FastME 2.0: A Comprehensive, Accurate, and Fast Distance-Based Phylogeny Inference Program. Molecular Biology and Evolution. 2015;32:2798–800.

148. Choi JY, Zaidem M, Gutaker R, Dorph K, Singh RK, Purugganan MD. The complex geography of domestication of the African rice Oryza glaberrima. PLOS Genetics. 2019;15:e1007414.

## Figure Legend

**Figure 1. Dot plot comparing the assembly contigs of Basmati 334 and Dom Sufid** to (A) all chromosomes of the Nipponbare genome assembly and (B) only chromosome 6 of Nipponbare. Only alignment blocks with greater than 80% overlap in sequence identity are shown.

**Figure 2. *Circum*-basmati gene sequence evolution**. (A) The deletion frequency of genes annotated from the Basmati 334 and Dom Sufid genomes. Frequency was estimated from sequencing data on a population of 78 *circum*-basmati varieties. (B) Groups of orthologous and paralogous genes (*i.e.*, orthogroups) identified in the reference genomes of N22, Nipponbare (NPB), and R498, as well as the *circum*-basmati genome assemblies Basmati 334 (B334) and Dom Sufid (DS) of this study. (C) Visualization of the genomic region orthologous to the Nipponbare gene Os03g0418600 (*Awn3-1*) in the N22, Basmati 334, and Dom Sufid genomes. Regions orthologous to *Awn3-1* are indicated with a dotted box.

**Figure 3. Presence/absence variation across the *circum*-basmati rice genome assemblies**. (A) Distribution of presence/absence variant sizes compared to the japonica Nipponbare reference genome. (B) Number of presence/absence variants that are shared between or unique for the *circum*-basmati genomes. (C) Chromosome-wide distribution of presence/absence variation for each *circum*-basmati rice genome, relative to the Nipponbare genome coordinates.

**Figure 4. Repetitive DNA landscape of the Basmati 334 and Dom Sufid genomes**. (A) Proportion of repetitive DNA content in the *circum*-basmati genomes represented by each repeat family. (B) Distribution of insert times for the *gypsy* and *copia* LTR retrotransposons. (C)

Phylogeny of *gypsy* and *copia* LTR retrotransposons based on the *rve* gene. LTR retrotransposons were annotated from the reference genomes of domesticated and wild rices.

**Figure 5. Comparative genomic analysis of *circum*-basmati rice evolution**. (A) Maximum-likelihood tree based on four-fold degenerate sites. All nodes had over 95% bootstrap support. (B) Percentage of genes supporting the topology involving japonica (J; Nipponbare, NPB), *circum*-basmati (cB, *circum*-basmati; Basmati 334, B334; Dom Sufid, DS), and *O. rufipogon* (R) after an Approximately Unbiased (AU) test. (C) Results of ABBA-BABA tests. Shown are median Patterson's D-statistics with 95% confidence intervals determined from a bootstrapping procedure. For each tested topology the outgroup was always *O. barthii*. (D) Percentage of genes supporting the topology involving *circum*-aus (cA; N22), *circum*-basmati, and indica (I; R498) after an Approximately Unbiased (AU) test. (E) Per-chromosome distribution of D-statistics for the trio involving R498, N22, and each *circum*-basmati genome. Genome-wide D-statistics with 95% bootstrap confidence intervals are indicated by the dark and dotted lines. (F) Model of admixture events that occurred within domesticated Asian rice. The direction of admixture has been left ambiguous as the ABBA-BABA test cannot detect the direction of gene flow. The *Oryza sativa* variety groups are labeled as *circum*-aus (cA), *circum*-basmati (cB), indica (I), and japonica (J), and the wild relative is *O. rufipogon* (R).

**Figure 6. Population relationships among the *circum*-aus (cA), *circum*-basmati (cB), and japonica rices (J)**. (A) Sum of genome-wide topology weights for a three-population topology involving trios of the *circum*-aus, *circum*-basmati, and japonica rices. Topology weights were estimated across windows with 100 SNPs. (B) Chromosomal distributions of topology weights

involving trios of the *circum*-aus, *circum*-basmati, and japonica rices (left), and the sum of the topology weights (right). (C) Best-fitting $\delta a \delta i$ model for the *circum*-aus, *circum*-basmati, and japonica rices. See Supplemental Table 17 for parameter estimates.

**Figure 7. Population structure within the *circum*-basmati rices**. (A) PCA plot for the 78-variety *circum*-basmati rice population genomic dataset. The three genetic groups designated by this study can be seen in the color-coded circles with dashed lines. (B) *ADMIXTURE* plot of K=2, 3, 4, and 5 for the 78 landraces. The color-coding from (A) is indicated above each sample's ancestry proportion. (C) Geographic distribution of the 78 *circum*-basmati rice varieties with their grouping status color-coded according to (A). (D) Agronomic measurements for the 78 *circum*-basmati rice varieties sorted into the three groups designated by this study. ** indicate p-value < 0.01 and *** indicate p-value < 0.001.

**Supplemental Figures**

**Supplemental Figure 1. Dot plot comparing chromosome 6 of japonica variety Nipponbare to *circum*-aus variety N22 and indica variety R498.**

**Supplemental Figure 2. Distribution of the proportion of missing nucleotides for japonica variety Nipponbare gene models across the orthologous non-japonica genomic regions.**

**Supplemental Figure 3. Effect of coverage threshold to call a deletion and the total number of deletion calls for samples with various genome coverage.**

**Supplemental Figure 4. Insertion time of LTR retrotransposon in various *Oryza* variety group genomes.** Number of annotated LTR retrotransposons is shown above boxplot. The variety group genomes that do not have a significantly different insertion time after a Tukey's range test are indicated with the same letter.

**Supplemental Figure 5. Density of presence-absence variation (PAV) per 500,000 bp window for each chromosome.**

**Supplemental Figure 6. Genome-wide topology weight from 500 SNP size window.** Chromosomal distribution of topology weights involving trios of the *circum*-aus, *circum*-basmati, and japonica rices (left), and the sum of the topology weights (right).

**Supplemental Figure 7. 13 demographic models tested by □a□i.**

**Supplemental Figure 8. □a□i model fit for the best-fitting demographic model.** Above row shows the observed and model fit folded site frequency spectrum. Below shows the map and histogram of the residuals.

**Supplemental Figure 9. Neighbor-joining phylogenetic tree of the 78 *circum*-basmati population sample.**

**Supplemental Table 1. Inversion detect by *sniffles* in the Nipponbare reference genome.**

**Supplemental Table 2. The 78 *circum*-basmati samples with Illumina sequencing result used in this study.**

**Supplemental Table 3. Names of the Basmati 334 and Dom Sufid genome gene models that had a deletion frequency of zero across the population.**

**Supplemental Table 4. Names of the Basmati 334 and Dom Sufid genome gene models that had a deletion frequency of above 0.3 and omitted from down stream analysis.**

**Supplemental Table 5. Orthogroup status for the Basmati 334, Dom Sufid, R498, Nipponbare, and N22 genome gene models.**

**Supplemental Table 6. Count and repeat types of the presence-absence variation (PAV) in the Basmati 334 or Dom Sufid genome in comparison to the Nipponbare genome.**

**Supplemental Table 7. Gene ontology results for orthogroups where gene members from the *circum*-basmati are missing.**

**Supplemental Table 8. Gene ontology results for orthogroups where gene members from *circum*-aus, indica, and japonica are missing.**

**Supplemental Table 9. Population frequency across the 78 *circum*-basmati samples for orthogroups that were specifically missing a gene in the Basmati 334 and Dom Sufid**

**genome gene models.**

**Supplemental Table 10. Genome coordinates of the LTR retrotransposons of the Basmati 334 genomes.**

**Supplemental Table 11. Genome coordinates of the LTR retrotransposons of the Dom Sufid genomes.**

**Supplemental Table 12. Genome coordinates of the Gypsy elements indicated with a single star in Figure 3.**

**Supplemental Table 13. Genome coordinates of the Copia elements indicated with a single star in Figure 3.**

**Supplemental Table 14. Genome coordinates of the Gypsy elements indicated with a double star in Figure 3.**

**Supplemental Table 15. Genome coordinates of the Copia elements indicated with a triple star in Figure 3.**

**Supplemental Table 16. The 82 *Oryza* population samples with Illumina sequencing result used in this study.**

**Supplemental Table 17. □a□i parameter estimates for the 13 different demographic models.** See supplemental figure 7 for visualization of the estimating parameters.

A

Nipponbare Chromosome

Basmati 334 Assembly

Dom Sufid Assembly



B

Nipponbare Chromosome 6

Basmati 334 Assembly

Dom Sufid Assembly

A

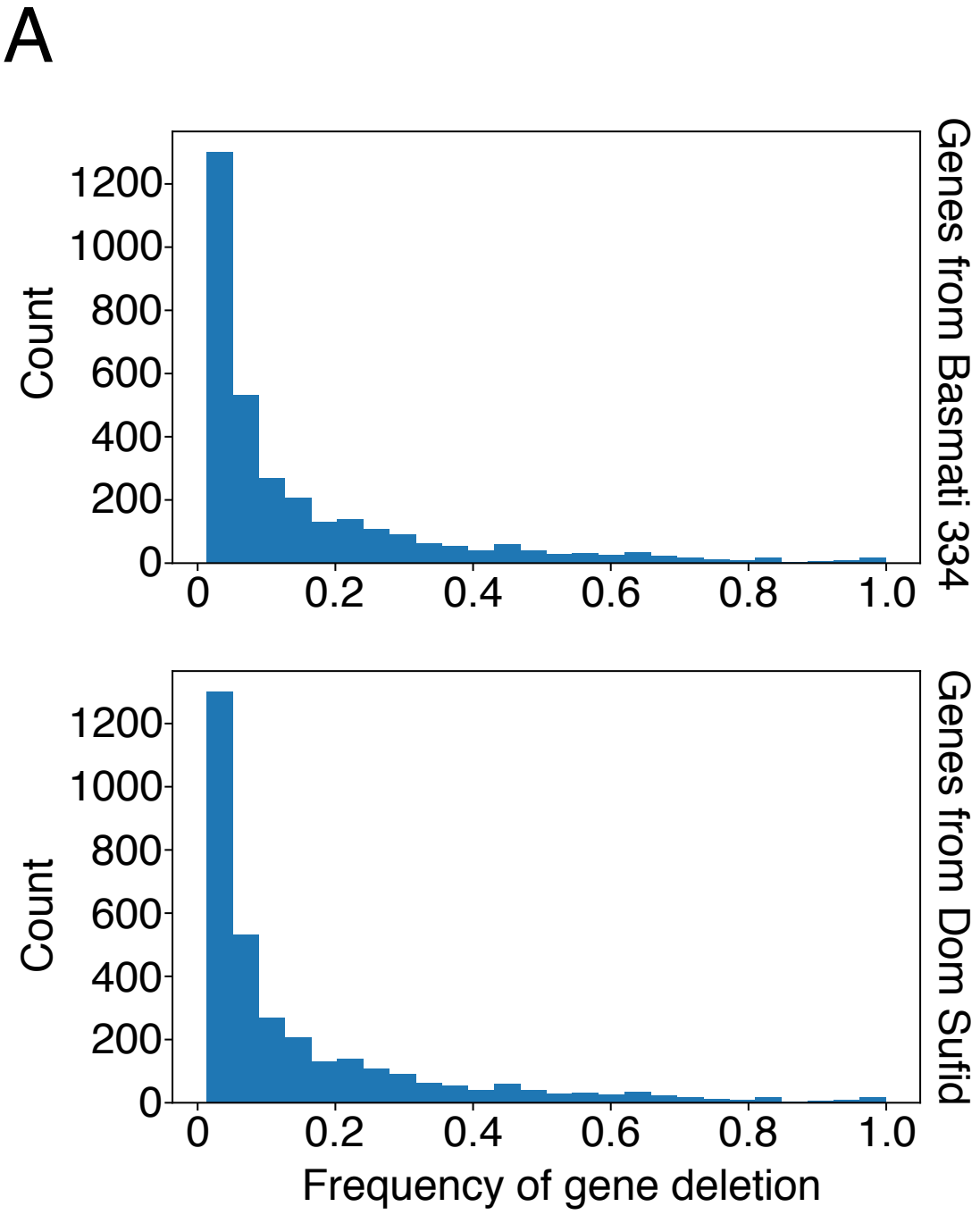


C

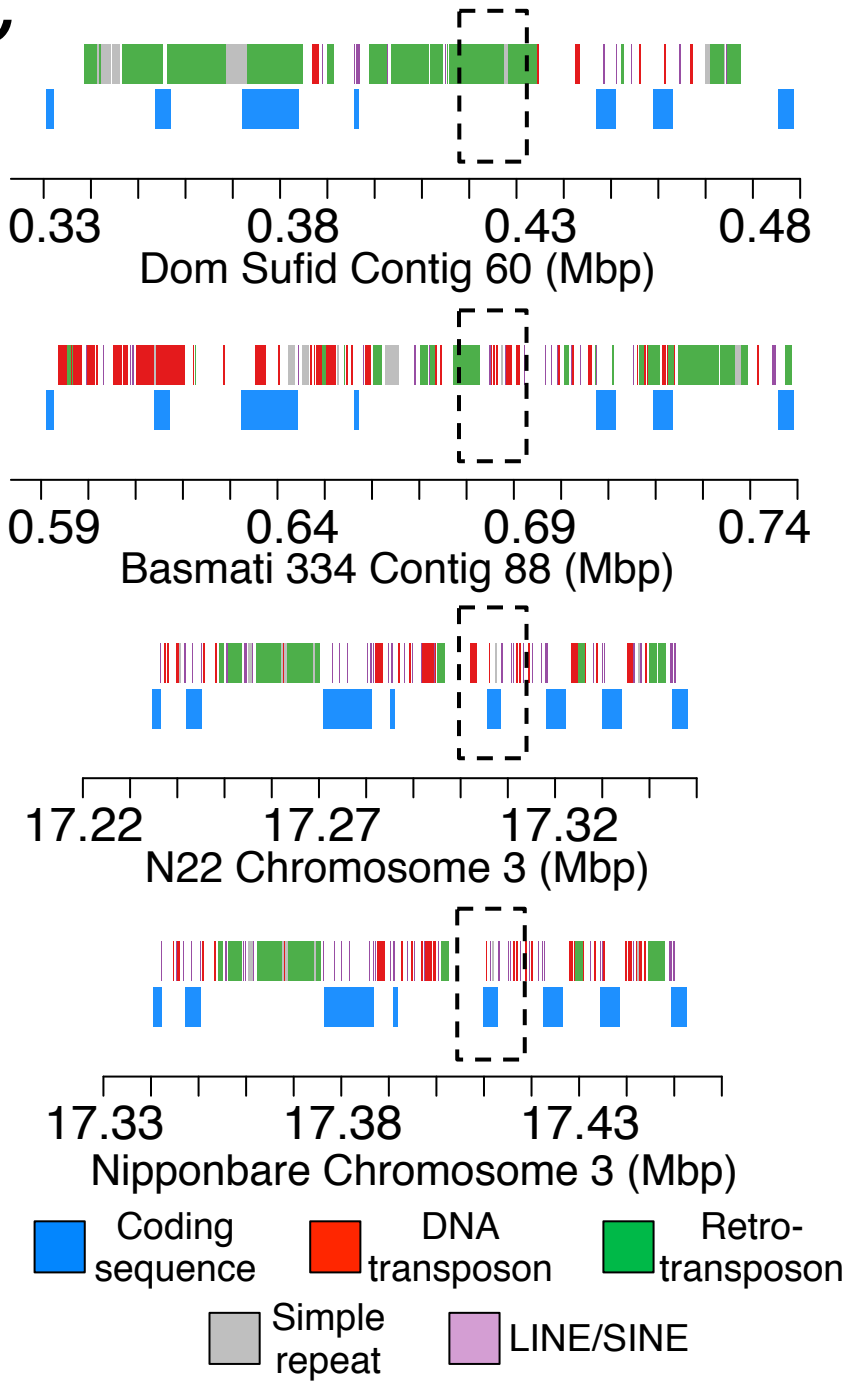


B

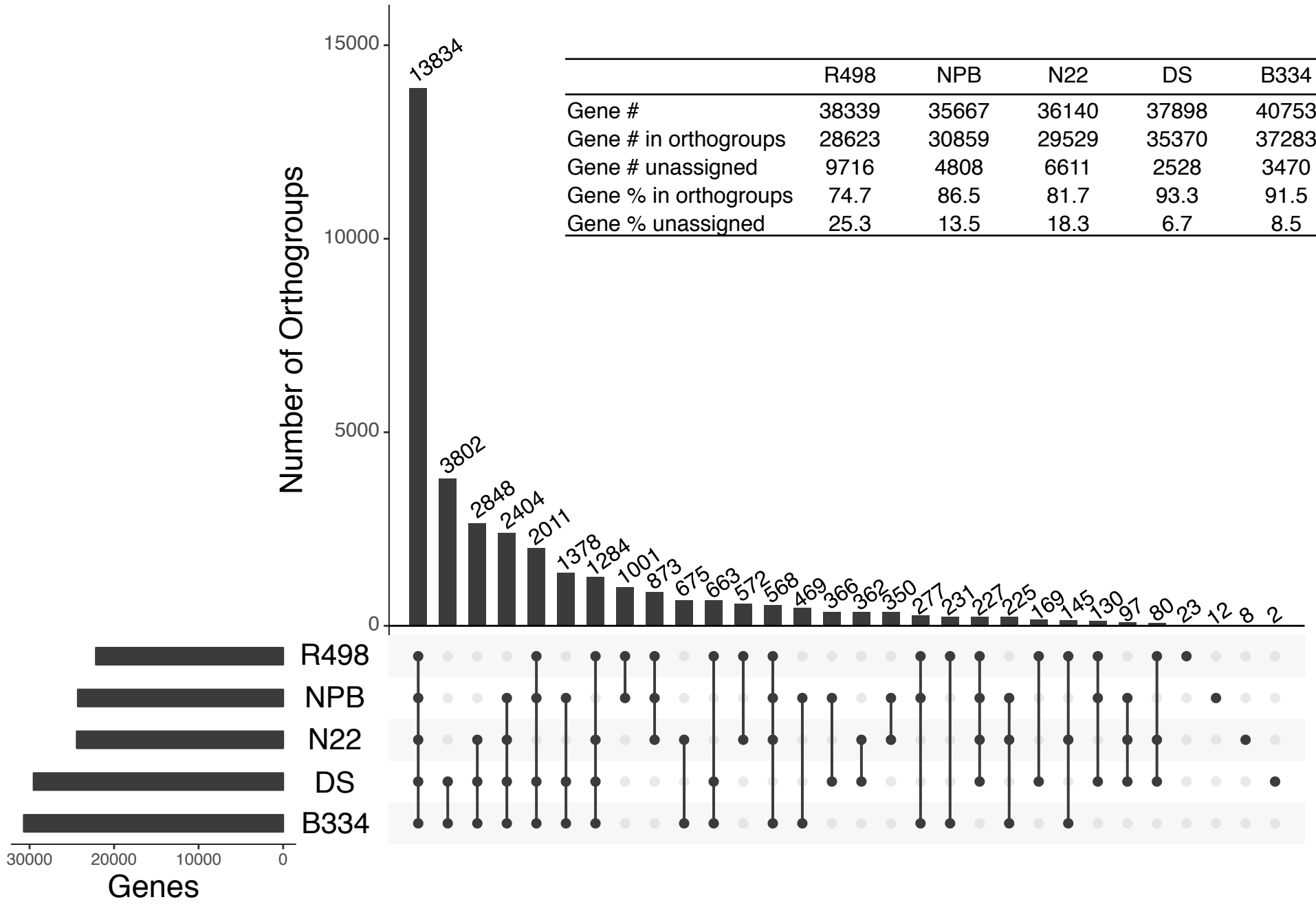


| | R498 | NPB | N22 | DS | B334 |
|---|---|---|---|---|---|
| Gene # | 38339 | 35667 | 36140 | 37898 | 40753 |
| Gene # in orthogroups | 28623 | 30859 | 29529 | 35370 | 37283 |
| Gene # unassigned | 9716 | 4808 | 6611 | 2528 | 3470 |
| Gene % in orthogroups | 74.7 | 86.5 | 81.7 | 93.3 | 91.5 |
| Gene % unassigned | 25.3 | 13.5 | 18.3 | 6.7 | 8.5 |

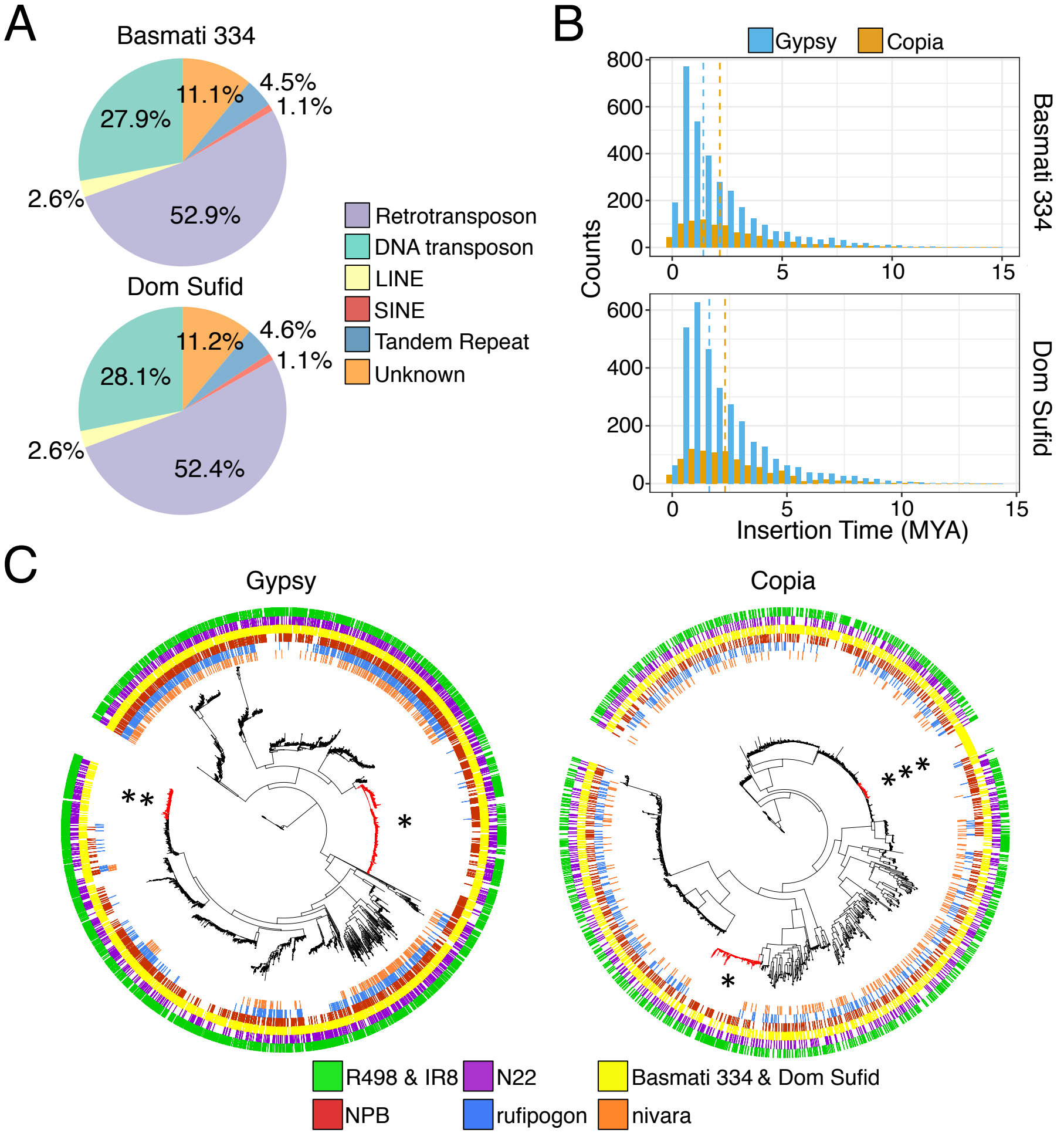
A
Basmati 334
11.1%
4.5%
1.1%
27.9%
2.6%
52.9%
Dom Sufid
11.2%
4.6%
1.1%
28.1%
2.6%
52.4%
Retrotransposon
DNA transposon
LINE
SINE
Tandem Repeat
Unknown
B
Gypsy
Copia
Counts
Basmati 334
Dom Sufid
Insertion Time (MYA)
C
Gypsy
Copia
R498 & IR8
N22
Basmati 334 & Dom Sufid
NPB
rufipogon
nivara

A

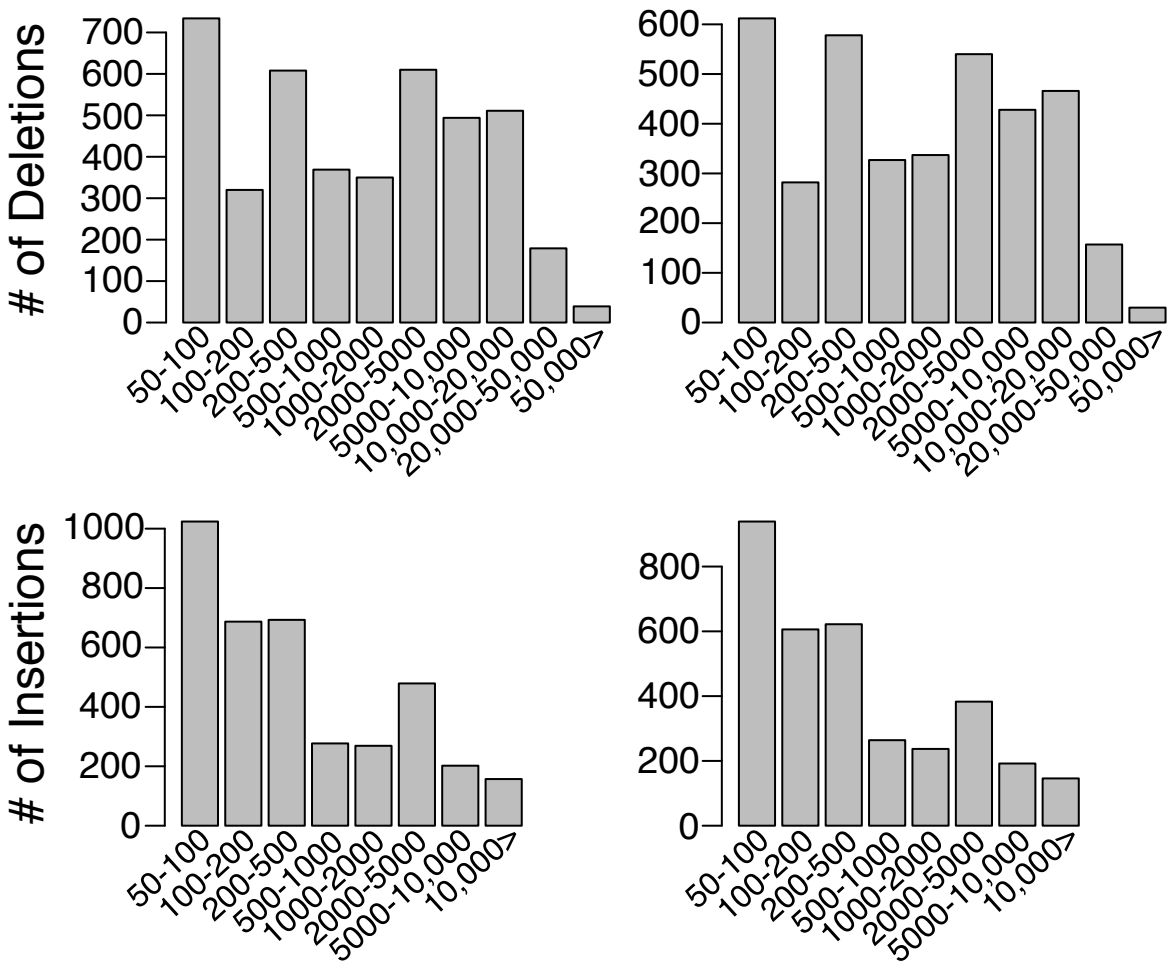
Basmati 334
Dom Sufid
# of Deletions
# of Insertions
50-100
100-200
200-500
500-1000
1000-2000
2000-5000
5000-10,000
10,000-20,000
20,000-50,000
50,000>
10,000>
Size of INDEL (bp)

B

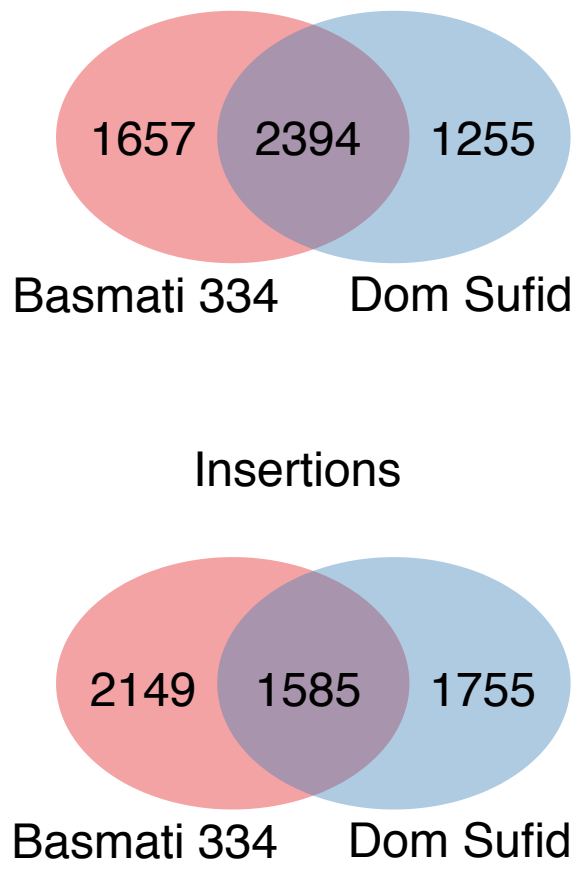
Deletions
1657
2394
1255
Basmati 334
Dom Sufid
Insertions
2149
1585
1755
Basmati 334
Dom Sufid

C

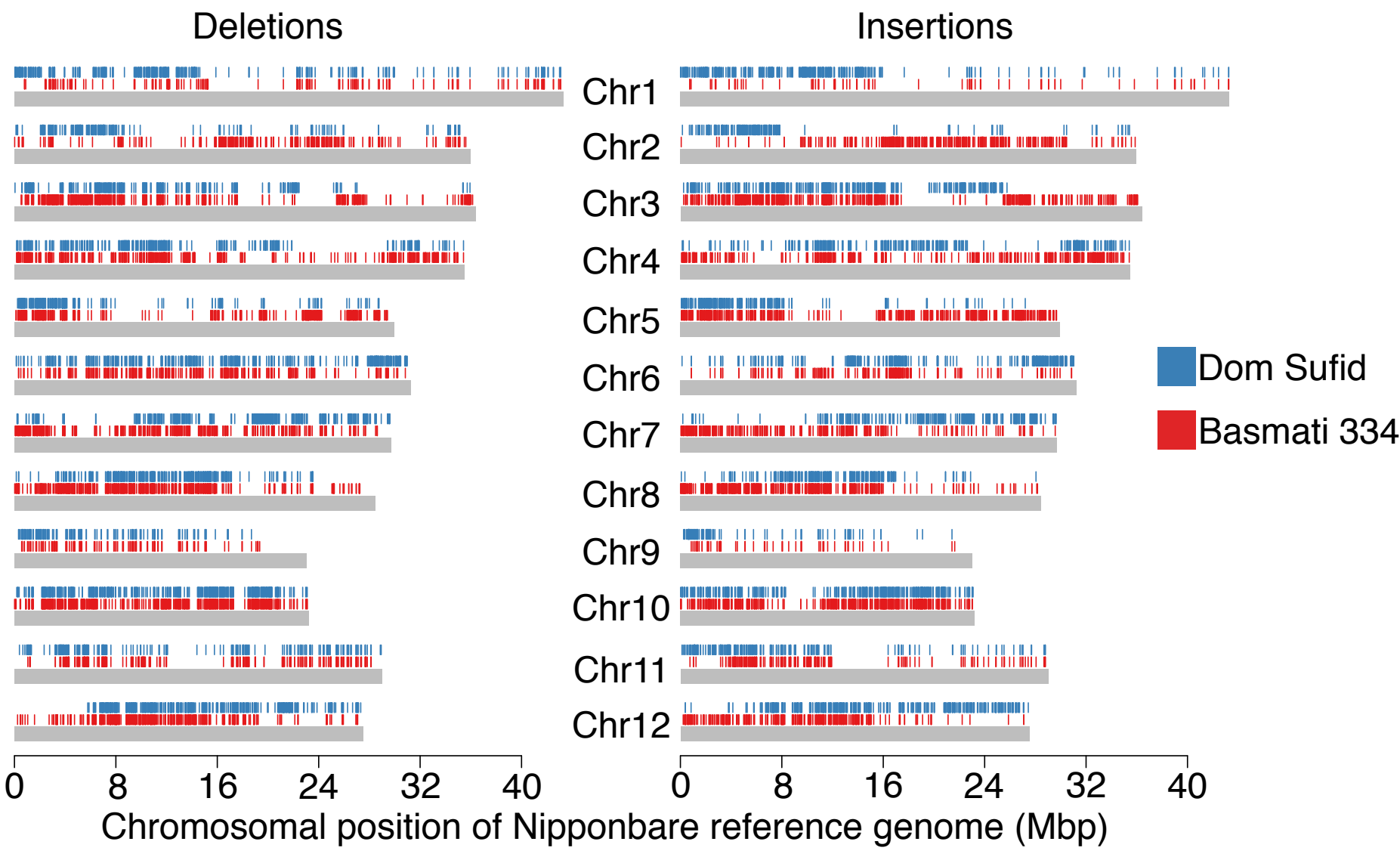
Deletions
Insertions
Chr1
Chr2
Chr3
Chr4
Chr5
Chr6
Chr7
Chr8
Chr9
Chr10
Chr11
Chr12
Dom Sufid
Basmati 334
0
8
16
24
32
40
Chromosomal position of Nipponbare reference genome (Mbp)

A

0.001

barthii

$J_{NPB}$

rufipogon

$cB_{DS}$

$cB_{B334}$

$I_{ZS97}$

$I_{IR8}$

$I_{IR64}$

$I_{MH63}$

$I_{R498}$

$cA_{N22}$

$cA_{DJ123}$

nivara

F

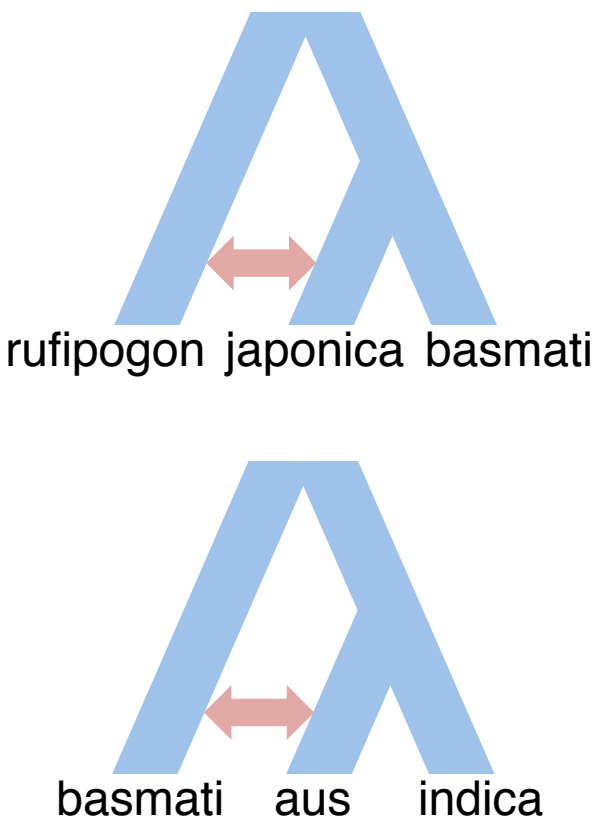


B

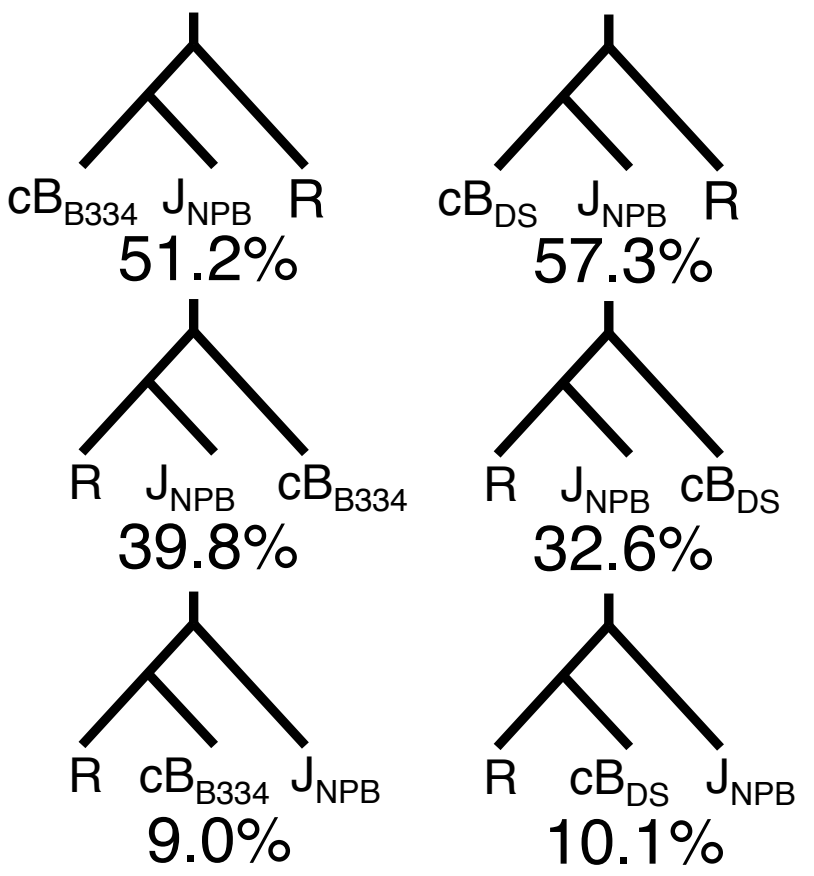


C

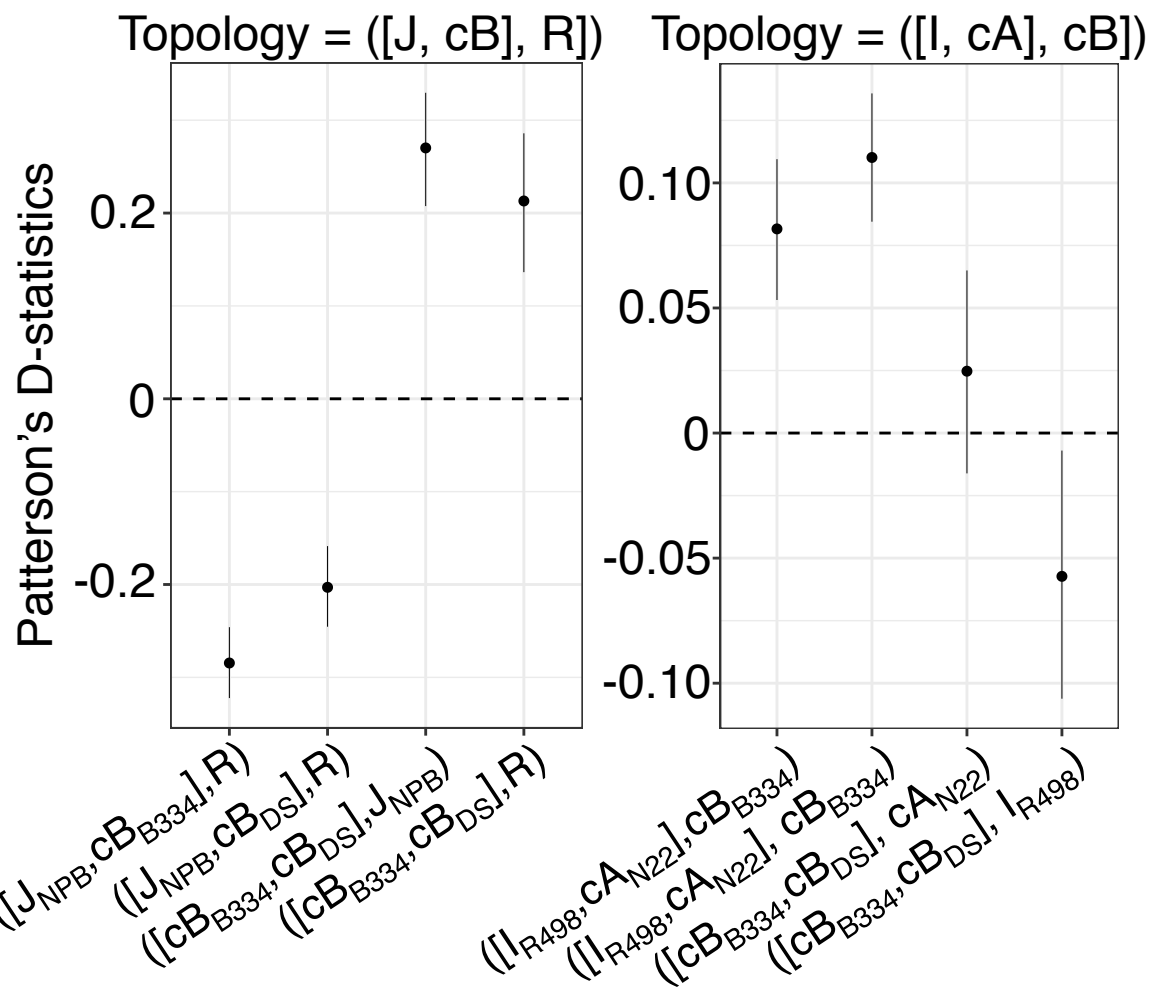


D

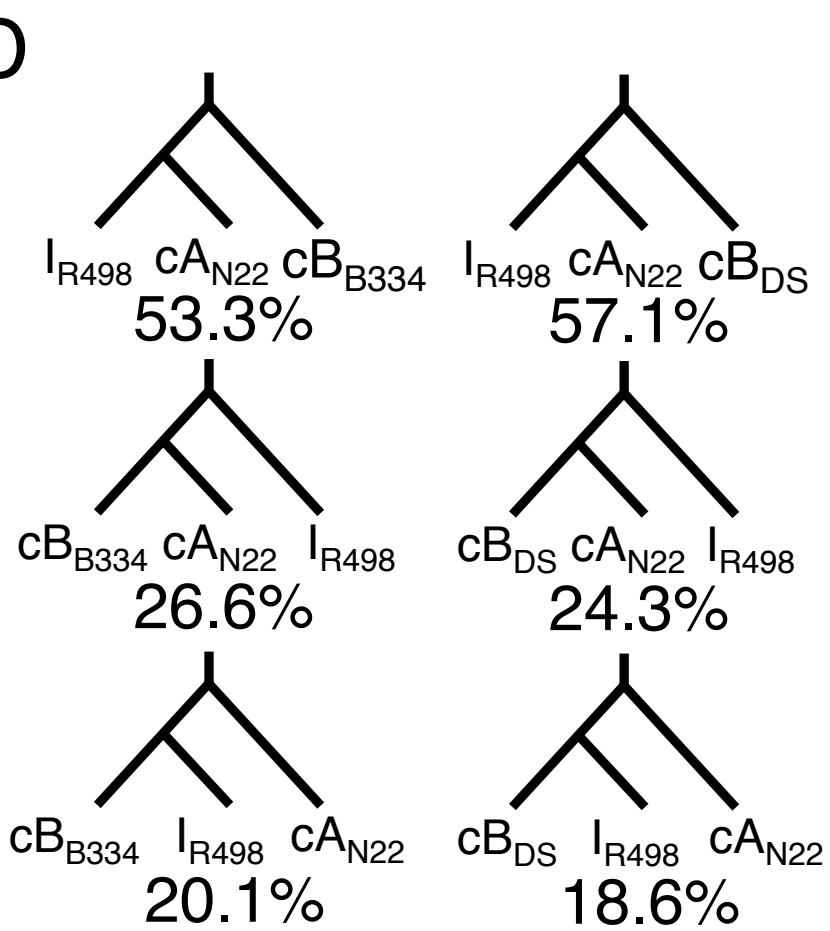


E

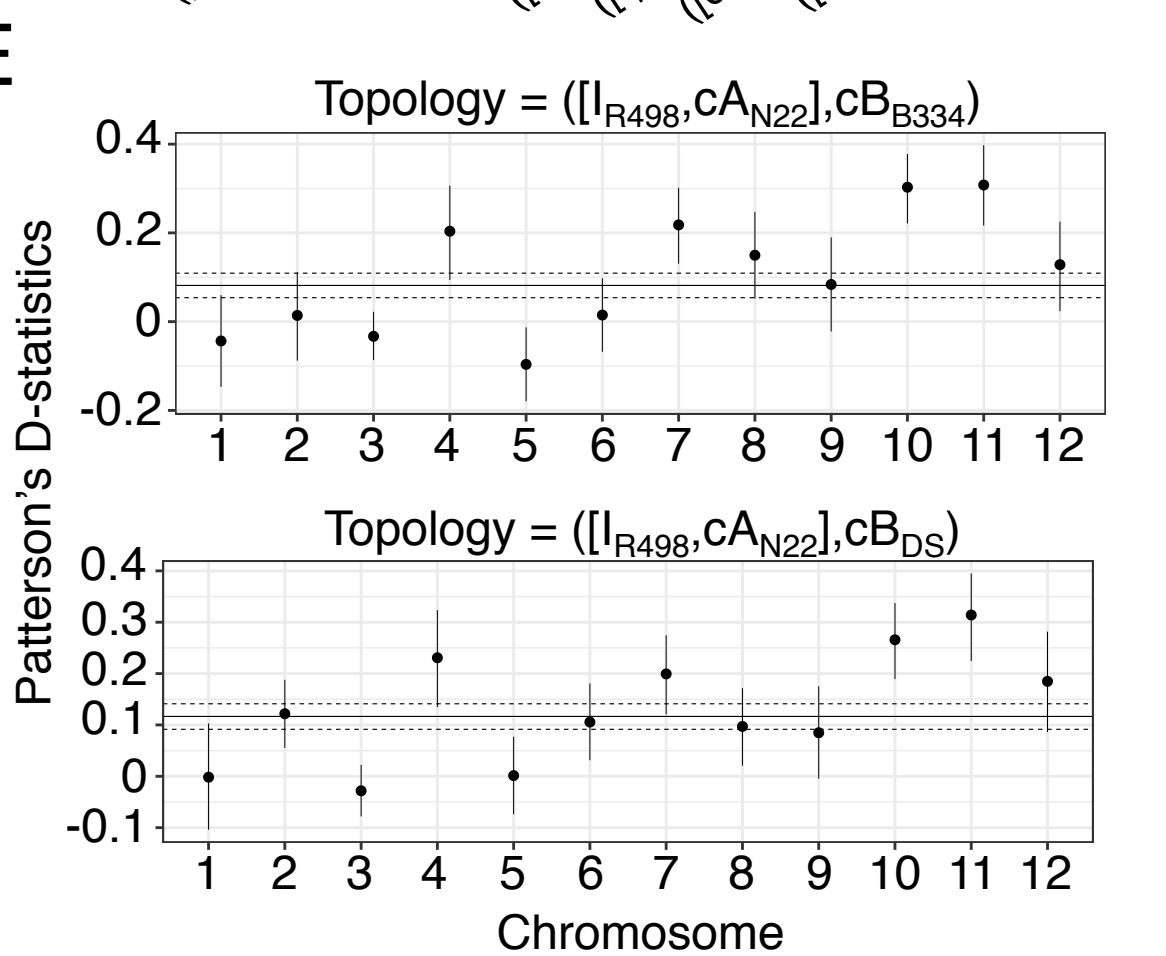

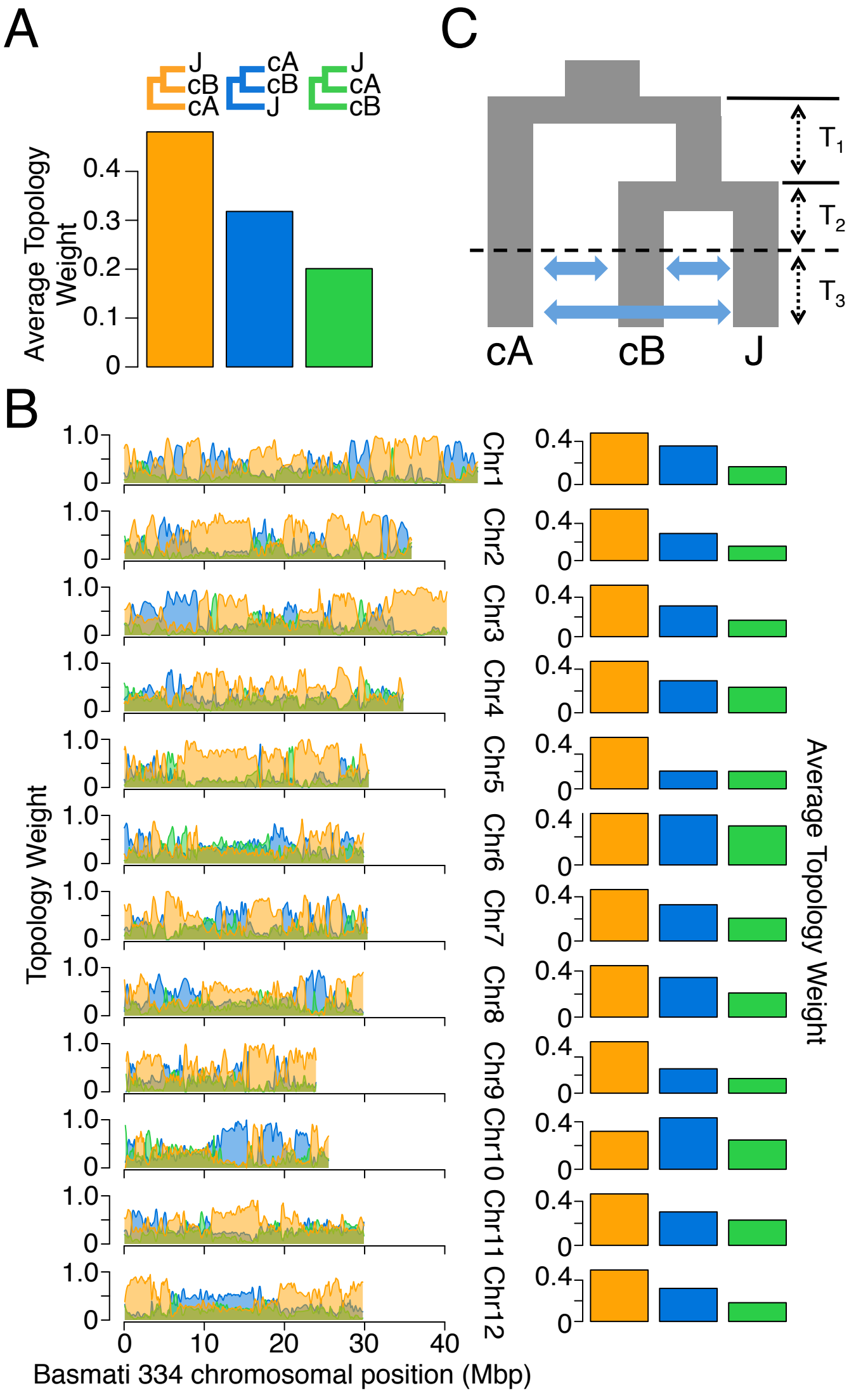
A
J
cB
cA
cA
cB
J
J
cA
cB
Average Topology Weight
0.4
0.3
0.2
0.1
0
C
T1
T2
T3
cA
cB
J
B
Topology Weight
1.0
0
Chr1
Chr2
Chr3
Chr4
Chr5
Chr6
Chr7
Chr8
Chr9
Chr10
Chr11
Chr12
0.4
0
Average Topology Weight
0
10
20
30
40
Basmati 334 chromosomal position (Mbp)

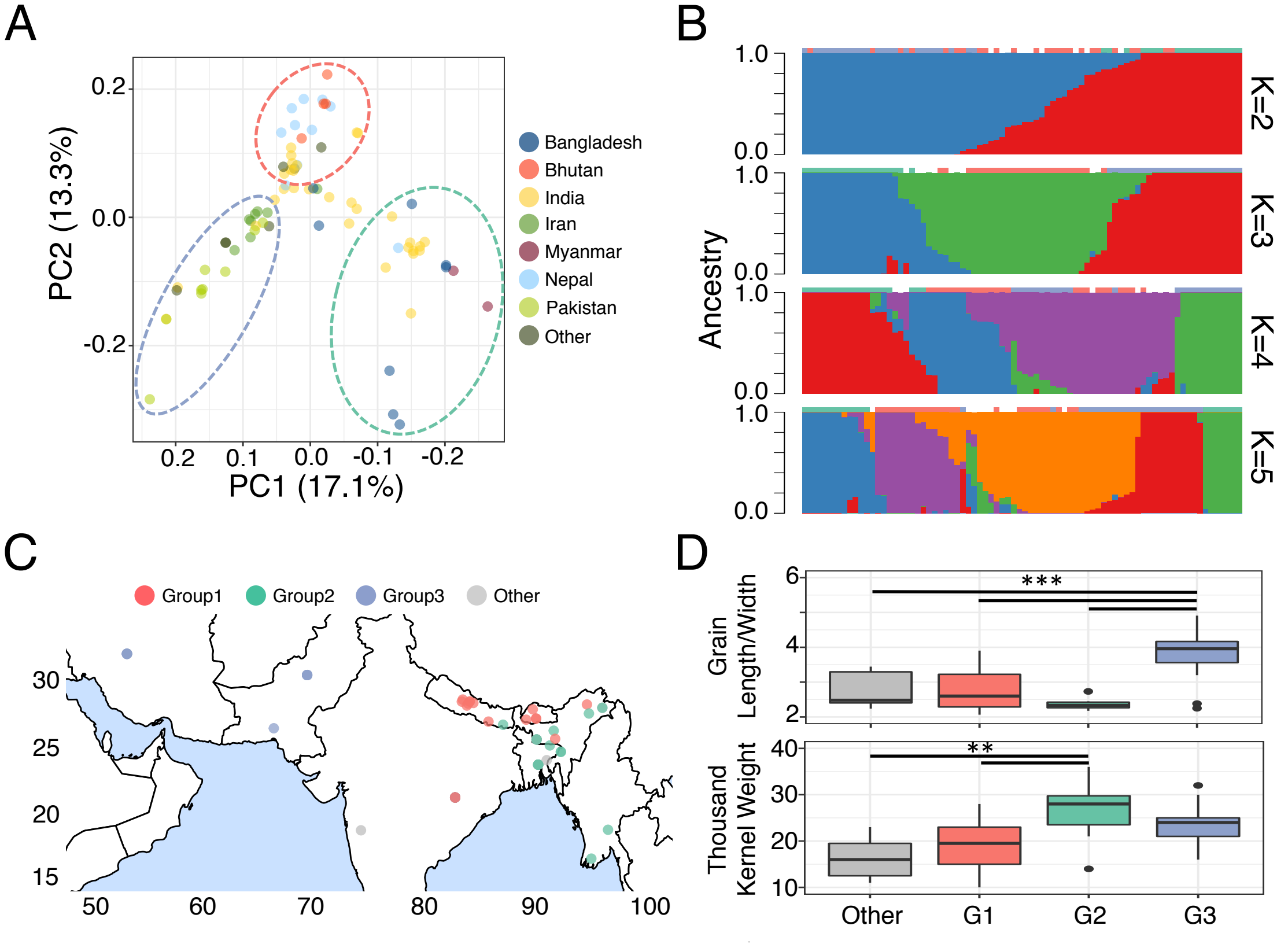
A
PC2 (13.3%)
PC1 (17.1%)
0.2
0.0
-0.2
0.2
0.1
0.0
-0.1
-0.2
Bangladesh
Bhutan
India
Iran
Myanmar
Nepal
Pakistan
Other
B
Ancestry
1.0
0.0
K=2
K=3
K=4
K=5
C
Group1
Group2
Group3
Other
30
25
20
15
50
60
70
80
90
100
D
Grain Length/Width
***
6
4
2
Thousand Kernel Weight
**
40
30
20
10
Other
G1
G2
G3